הטכניון
מכון טכנולוגי לישראל
TECHNION
Israel Institute of Technology

ספריות הטכניון
The Technion Libraries

בית הספר ללימודי מוסמכים ע"ש ארווין וג'ואן ג'ייקובס
Irwin and Joan Jacobs Graduate School

Bearing-only Formation Control with Directed Sensing

Research Thesis
In Partial Fulfillment of The Requirement
for the Degree of Master of Science in
Autonomous Systems and Robotics

Jiacheng Shi

Submitted to the Senate
of the Technion - Israel Institute of Technology
Haifa
Nissan 5784, April 2024

The Research Thesis Was Done in Autonomous Systems and Robotics Under the Supervision of Prof. Daniel Zelazo, in the Faculty of Aerospace Engineering.

The author of this thesis states that the research, including the collection, processing and presentation of data, addressing and comparing to previous research, etc., was done entirely in an honest way, as expected from scientific research that is conducted according to the ethical standards of the academic world. Also, reporting the research and its results in this thesis was done in an honest and complete manner, according to the same standards.

The generous financial help of the Technion is gratefully acknowledged.

Abstract

This thesis investigates the formation control problem, which aims to drive a multi-agent system to achieve a desired spatial configuration. A control scheme called bearing-only formation control is proposed to solve this problem. This controller has attracted research interest because it requires and applies only bearing measurements between agents, rather than using distance measurements.

One limitation of bearing-only formation control is the sensing condition assumed. Early works extensively studied this controller assuming undirected sensing between agents, which is regarded as an unrealistic condition. More recent efforts have focused on the problem with directed sensing, where agent i can sense agent j but not necessarily vice versa. Recent research showed that the bearing-only formation control law also works with a specific class of directed sensing graphs called leader-first-follower (LFF) graphs generated from a bearing-based Henneberg construction. This was a major step forward from the previous assumption of undirected graphs to a limited class of directed graphs. Building on this, the goal of this work is to extend the results to more general conditions on the directed sensing graphs for which bearing-only formation control succeeds.

To achieve this, we first analyze a multi-agent system with one movable agent controlled by the bearing-only formation controller. The goal is to determine whether this movable agent will converge to a desired position satisfying all specified target bearings, for different numbers of outgoing edges (agents it can sense). The main challenge is finding equilibrium points of this nonlinear system. Our approach focuses on analyzing a related linear problem and establishing connections to equilibria of the nonlinear system. After determining the system equilibria, we also provide stability analysis showing that the movable agent converges to the desired position. This result then allows us to extend the class of graphs that solve the problem to LFF graphs where the follower agents can have more than 2 outgoing sensing edges. We provide stability and convergence analysis for this case. We also explore a further expansion of the class of graphs and conjecture that a sufficient condition for solving the more general formation control problem is that there must exist a subgraph that is a LFF graph. This conjecture is verified with simulation studies. Eventually, we conclude the general conditions for the directed graphs with which the bearing-only formation control works, which is the main contribution of this research.

Contents

List of Figures

Abbreviations and Notations

$\mathbb{R}$	: Set of real numbers
$\mathbb{R}^{m\times n}$	: Real matrix of dimension $m \times n$
$\mathbb{1}_n, \mathbb{0}_n$	: n-dimensional vector with all entries 1 or 0
I_n	: n-dimensional identity matrix
$\|\cdot\|$	: Euclidean norm
$\otimes$	: Kronecker product
MAS	: Multi-agent system
BOFC	: Bearing-only formation control
(HC)LFF	: Leader first-follower graph (generated from Henneberg construction)
(A)GAS	: (Almost) Global asymptotically stable
BR	: Bearing rigid
GBR	: Globally bearing rigid
IBR	: Infinitesimally bearing rigid

1 Introduction

Multi-agent system (MAS) has garnered substantial attention and research efforts in the control and robotics communities. A multi-agent system is defined to be a system composed of multiple autonomous agents interacting with each other to achieve common or individual goals. The agents are required to be capable of perceiving and acting upon the environment of the system. The unmanned aerial vehicles, software entities, robots and humans can be chosen as the agents.

Application of MAS can be found in different fields, for example in traffic and transportation [1], power engineering [2, 3], and chaos analysis [4]. The application as well as the theoretical improvement in controlling MAS is still a widely open question and the subject of active research. Formation control refers to the coordinated behavior exhibited by a group of autonomous entities, such as robots, drones, or vehicles, to achieve a desired geometric configuration or pattern. In formation control, agents or entities cooperate and adjust their positions relative. This coordination can be accomplished through numerous communication and control strategies, allowing the agents to align or maintain specific geometric relationships, such as maintaining a fixed distance or bearing angle.

Formation control has obtained significant attention across a wide range of fields, including robotics [5], autonomous systems, aerial and ground vehicle networks [6], and swarm robotics [7]. The study of formation control involves developing algorithms, control strategies, and communication protocols to enable the formation members to realize or maintain the desired formations. These formations can range from simple geometric shapes, such as circles or lines, to more complex configurations.

The information that agents communicate with each other is crucial for developing algorithms in formation control. The characterization of formation control schemes based on the sensing capability and the interaction topology leads to the problem of what variables can be sensed and what variables are actively controlled by MAS to achieve a desired formation. The types of formation control are specified by the variables which is required to be satisfied in the desired formation, such as the position-constrained formation control [8], the displacement-constrained formation control [9], distance-constrained formation control [10] and bearing-constrained formation control [11], which aims to control the system to some configurations fulfilling the displacement, distance or bearing constraints.

Meanwhile, the requirement of sensed variables are essentially connected to the interaction topology. Information can be obtained by local sensors or provided over a communication link to other agents or a centralized control unit. The local sensor usually provides the relative bearing or distance information with respect to other agents. Range sensors are able to receive relative distance information to objects around them. Visual sensors such as cameras are capable to collect the bearing information which is expressed as unit vectors. Limitation due to the effective working space exists on both range sensors and visual sensors. The limitations could

lead a sensing network not necessarily static or undirected. Note that undirected refers to the case where an agent can sense its neighbor but not the other way round. The global information for the agents are also available through a centralized control unit. It is unfeasible for the MAS reach some configurations defined in global framework with the relative information only. Specifically, if all the position information of individual agents can be sensed and controlled, the MAS can move to the desired positions without interaction. In the case that the positions of part of agents can be sensed, while only relative distance can be obtained for other agents, the interaction between these two types of agents should be essentially working to achieve the target formation. In short, the types of controlled variables specify the best possible desired formation that can be achieved by agents, which in turn prescribes the requirement on the interaction topology of the agents.

1.1 Literature Review

In this section, we will review the existing works dealing with bearing-only formation control to cover the basic foundation and motivation of our work. Then, we will also discuss the development on bearing rigidity theory, which acts an important role in bearing-constrained formation control problem.

Bearing-only formation control.

In formation control, the core problem is to design the distributed control strategy for each agent such that the agents achieve and maintain a desired spatial arrangement or target formation. The distance-constrained formation control [12, 13, 14] takes the prominent role in early studies of formation control. Here, the target formations are specified using inter-agent distances. Most of the distance-constrained formation control [15, 16] requires relative position measurements between the agents. The bearing-constrained formation control [11, 17] has attracted more attention recently since the bearing measurement is often cheaper and more accessible than the position measurement. In the bearing-constrained formation control, the control algorithm is based on the bearing measurement and the target formation is defined by the inter-agent bearings.

Various control strategies have been developed in the field of bearing-constrained formation control. Some of the strategies made use of position measurement or distance measurement [18, 19], while other works utilized the bearing measurement to estimate the relative distance or positions [20]. A linear bearing-based control law [17] was proposed using bearing rigidity theory. It is a natural solution of formation control which stabilizes static target formations in arbitrary dimensions with undirected sensing. Many works then focus on developing the bearing-based formation control. In [21], the bearing-based formation control is applied to the maneuvering case where the leaders have nonzero constant velocities. It also contributes to the localization problem for bearing-based network [22]. The work [23] and [24] investigate bearing persistence problem which give certain conditions for when bearing-based formation control works with directed sensing.

One of the common properties of the control schemes mentioned in last paragraph is the requirement for different types of measurements. Due to the advantage of bearing measurements, most of the research efforts investigated control laws employing only bearing measurements. In the beginning, some works have addressed such control strategy considering a limited number of agents [25]. After then, the work [26] presented a control framework for a group of UAVs bound with the 3D bearing formation formally defined. The same author further investigated the relationship between scalability, minimality and rigidity, and proposed a distributed bearing-only control strategy stabilizing the bearing formation in [27].

Along with the development of bearing rigidity theory, the bearing-only formation control (BOFC) studied in this thesis was proposed in [11]. This control scheme is designed for agents modelled with single integrator dynamics. The communication between the agents is descried by an undirected sensing graph. The bearing measurements in the control system are defined in a global reference frame of arbitrary dimensions. The desired bearing formation composed of the undirected sensing graph and a desired bearing vector is required to be infinitesimally bearing rigid. They showed that the centroid and scale of the framework is invariant during the full motion. A target framework satisfying the desired bearing formation can be uniquely determined up to the initial centroid and scale. Most importantly, the bearing-only formation control can exponentially drive the MAS to the target framework from almost every initial condition.

It should be emphasised that the undirected sensing demanded in [11] is an unrealistic restriction. The work [28] demonstrates an instance that the sensing condition is more likely directed because of the limited field of view for bearing sensors. The research of bearing-only formation control with directed sensing graphs was firstly explored in [29]. They revealed that the directed sensing would bring asymmetry into the control system, with which the centroid and scale of the framework is no longer invariant. The analysis of convergence given for the undirected sensing case is also not feasible. With these challenges, they suggested a specific class of directed graph called the *leader first follower* graph generated from bearing-based Henneberg construction. With such directed sensing graphs, the resulting control strategy is shown to have a nonlinear cascade structure which is leveraged for the stability analysis, showing the system can asymptotically converge to the correct shape.

Bearing Rigidity Theory.

The bearing rigidity (or parallel rigidity) theory is a fundamental concept in the research of formation control, which deals with the rigid structures and their underlying geometric properties. In various engineering and scientific disciplines, understanding the rigidity of structures is of paramount importance. Rigidity refers to the property of a structure to maintain its shape and resist deformation under external forces. The bearing rigidity theorem provides a theoretical framework to determine whether a given structure, composed of interconnected elements, can retain its shape when subjected to different bearing measurements or angular constraints. The bearing rigidity theorem establishes conditions under which a structure can be

uniquely determined or reconstructed based solely on the relative angles or bearings between its constituent elements.

Bearing rigidity theory in two-dimensional space (also termed parallel rigidity) is explored in [30]. In [31], a formal characterization is stated for $SE(2)$ frameworks. Then, the theory has been extended to an arbitrary dimensional space for undirected graphs in [11]. The generically bearing rigidity in [32] demonstrates that the underlying graph acts a more important role than the configuration. The work [33] provides an approach on $SE(3)$ framework with directed graphs. Nonetheless, the bearing rigidity theory for directed graphs are still widely open.

1.2 Thesis Contribution

This thesis considers the bearing-only formation control problem with directed sensing. The previous work [29] showed that the bearing-only formation control drives the MAS to target formation if the directed sensing condition is a leader-first-follower graph generated from Henneberg construction, which is a special class of directed graphs. In this work, we aim to extend the directed sensing graphs to be more general.

The contribution begins with a simple system consisting of a movable agent and several fixed agents. The goal is to determine whether this movable agent will converge to a desired position satisfying all specified target bearings, for different numbers of outgoing edges (agents it can sense). As we will see further in this thesis, finding equilibrium points of the nonlinear system is the pivot of the work. Instead of looking for the equilibrium of nonlinear system, we focus on a related linear system and establish connections to equilibrium of the nonlinear system. The equilibrium of linear system is determined mainly by the null space analysis. Lastly, the stability is checked by Lyapunov functions.

The main contribution is the expansion of directed graphs. In the primary expansion, we add edges which keep the cascade structure in control system. By the stability theorem of cascade system, we are able to analyze the convergence of the control system step by step. In the procedure, the result of the simple system can be applied. Then, a further expansion of the class of graphs is proposed. A sufficient condition for solving the more general formation control problem is that there must exist a subgraph that is a LFF graph. The equilibrium of the nonlinear system related with the further expanded sensing graph is determined with the similar trick as the simple system. A conjecture on the stability of the equilibrium is proposed and verified with simulation results.

1.3 Thesis Organization

The thesis is organized as follows. In Chapter 2, we present a background on graph theory, bearing rigidity theory and the bearing-only formation control with undirected sensing and specific directed sensing. In Chapter 3, we firstly motivate the graph expansion with a few numerical simulations. A simple system is analyzed to built the basis of determining the equilibrium of nonlinear control system. After

then, we suggest some classes of graphs generalized from the HCLFF graph and show how the bearing-only formation control works with the corresponding directed sensing. In Chapter 4, the conclusion and direction for future works is given.

2 Preliminaries

In this section, some basic definitions and theorems on graph theory and stability theory will be reviewed. On the other hand, we will also introduce the primary control strategy in this thesis, the bearing-only formation controller.

2.1 Graphs and the Theory of Rigidity

Graph theory is the study of graphs, which are mathematical structures modelling the relation between objects. In a graph, objects are always expressed as nodes and the relationships are translated as edges. In this section, we will first give the notations and definitions used to describe graphs [34], and then introduce the theory of bearing rigidity [11], a central concept used in bearing formation control.

Graph Theory.

In mathematics, graphs are mathematical structures used to model pairwise relations between objects. Generally, a graph, denoted $\mathcal{G} = (\mathcal{V}, \mathcal{E})$, consists of a non-empty finite set $\mathcal{V}$ called the *vertex set*, and a finite set $\mathcal{E}$ of pairs of distinct elements in $\mathcal{V}$, called *edge set*. The elements in vertex set $\mathcal{V} = \{v_1, \cdots, v_n\}$ are called the *vertices* (or nodes) of the graph $\mathcal{G}$. The size of the vertex set $|\mathcal{V}| = n$ coincides with the number of vertices.

A graph can be classified as *undirected* or *directed*. In the undirected graph, the edge set $\mathcal{E}$ are composed of edges without orientation. The undirected edge denoted as $e_{ij} = \{v_i, v_j\}$ connects the agent v_i and v_j, implying these two agents are in the neighbourhood of each other, which is notated as $v_i \in \mathcal{N}_j, v_j \in \mathcal{N}_i$. In directed graphs, the edge set $\mathcal{E}$ is consisted of edges with orientations. The notation for a directed edge is $e_{ij} = (v_i, v_j)$ indicates that the edge starts from agent v_i and end at agent v_j. The appearance of the directed edge e_{ij} indicates that agent v_j is in the neighbourhood of agent v_i (i.e., $v_j \in \mathcal{N}_i$). Overall, the size of the edge set $|\mathcal{E}| = m$ coincides with the number of edges. For a graph $\mathcal{G} = (\mathcal{V}, \mathcal{E})$, either undirected or directed, a label can be assigned to each edge. If the edge $e_{ij} \in \mathcal{E}$ is labeled as the kth edge in the edge set, we may denote e_{ij} as e_k.

An example of an undirected graph and a directed graph is shown in Figure 1.

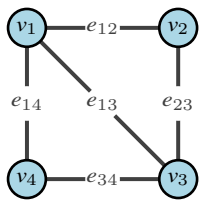

(a) An undirected graph.

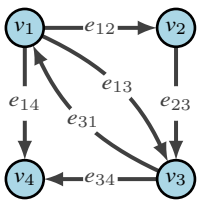

(b) A directed graph.

Figure 1: Example of a directed and undirected graph.

Both graphs share the same vertex set $\mathcal{V} = \{v_1, v_2, v_3, v_4\}$. The edge set for the undirected graph is

$$\mathcal{E}_{1a} = \{\{v_1, v_2\}, \{v_2, v_3\}, \{v_3, v_4\}, \{v_1, v_4\}, \{v_1, v_3\}\} = \{e_{12}, e_{23}, e_{34}, e_{14}, e_{13}\}.$$

In comparison, the edge set for the directed graph is composed of directed edges

$$\mathcal{E}_{1b} = \{(v_1, v_2), (v_2, v_3), (v_3, v_4), (v_1, v_4), (v_1, v_3), (v_3, v_1)\} = \{e_{12}, e_{23}, e_{34}, e_{14}, e_{13}, e_{31}\}.$$

Graphs may also be represented by appropriately defined matrices. Of interest to this work is the *incidence* matrix and *out incidence* matrix.

The incidence matrix of a graph, encoding the relation between edges and vertices, denoted as $H(\mathcal{G}) \in \mathbb{R}^{m \times n}$, is defined as

$$H(\mathcal{G})_{ki} = \begin{cases} 1, & \text{node } i \text{ is positive end of edge } e_k \\ -1, & \text{node } i \text{ is negative end of edge } e_k \\ 0, & \text{otherwise.} \end{cases} \tag{1}$$

A positive end is where the edge starts and the negative end is the terminal. For undirected graphs with undirected edges, the orientation should be assigned arbitrarily. By construction, the incidence matrix has exactly one 1 and -1 in each row. Thus, the all ones vector $\mathbb{1}_n$ is always in the null space of $H(\mathcal{G})$. Similarly, the *out-incidence* matrix, denoted as $H_{out}(\mathcal{G}) \in \mathbb{R}^{m \times n}$, is defined by directed graphs:

$$H_{out}(\mathcal{G})_{ki} = \begin{cases} 1, & \text{node } i \text{ is positive end of edge } e_k \\ 0, & \text{otherwise.} \end{cases}. \tag{2}$$

Reconsider the example of directed graph (Fig. 1b). The order of edges is set as

$$\{e_{12}, e_{23}, e_{34}, e_{41}, e_{13}, e_{31}\} \rightarrow \{e_1, e_2, e_3, e_4, e_5, e_6\},$$

then the incidence matrix and out-incidence matrix of the graph can be expressed as

$$H = \begin{bmatrix} 1 & -1 & 0 & 0 \\ 0 & 1 & -1 & 0 \\ 0 & 0 & 1 & -1 \\ 1 & 0 & 0 & -1 \\ 1 & 0 & -1 & 0 \\ -1 & 0 & 1 & 0 \end{bmatrix}, \; H_{out} = \begin{bmatrix} 1 & 0 & 0 & 0 \\ 0 & 1 & 0 & 0 \\ 0 & 0 & 1 & 0 \\ 1 & 0 & 0 & 0 \\ 1 & 0 & 0 & 0 \\ 0 & 0 & 1 & 0 \end{bmatrix}. \tag{3}$$

Frameworks and Formations.

The central work of rigidity theory is to determine the flexibility or rigidity of a structure, which is mathematically described with a framework. So in this section, we firstly review the construction of a *framework*.

A framework in $\mathbb{R}^{\mathsf{d}}$, denoted as $(\mathcal{G}, p)$, consists of a graph $\mathcal{G} = (\mathcal{V}, \mathcal{E})$ and a configuration $p = [p_1^T, \cdots, p_n^T]^T \in \mathbb{R}^{\mathsf{d}n}$. The framework $(\mathcal{G}, p)$ is actually formed by mapping the vertex $v_i \in \mathcal{V}$ to the position $p_i \in \mathbb{R}^{\mathsf{d}}$. In a framework $(\mathcal{G}, p)$, the displacement vector between p_i and p_j is defined as $z_{ij} = p_j - p_i$ while its norm $d_{ij} = \|z_{ij}\|$ is denoted as the distance. The relative bearing vector $g_{ij} \in \mathbb{R}^{\mathsf{d}}$ is defined as the unit vector with the direction from p_i to p_j, which can be expressed as:

$$g_{ij} = \frac{z_{ij}}{\|z_{ij}\|} = \frac{p_j - p_i}{\|p_j - p_i\|}. \tag{4}$$

The displacement measurement z_{ij}, distance measurement d_{ij} and bearing measurement g_{ij} shows different relations between p_i and p_j. For all $v_i, v_j \in \mathcal{V}$, we call the measurement between agents as an *inter-agent measurement*. In addition, if $(v_i, v_j) \in \mathcal{E}$, or equivalently, $v_j \in \mathcal{N}_i$, we call the measurement from v_i to v_j as an *inter-neighbour measurement*. For any inter-neighbour measurement z_{ij}, d_{ij}, or g_{ij}, it can be related to the edge e_{ij}. Recall that the edge e_{ij} can also expressed by e_k according to its order. In the same way, the notation z_k, d_k, or g_k is given to the inter-neighbour measurement corresponding to the edge e_k.

When a framework $(\mathcal{G}, p)$ is constructed, the inter-neighbour bearing measurement can be generated by the bearing function $F_B : \mathbb{R}^{\mathsf{d}n} \to \mathbb{R}^{\mathsf{d}m}$,

$$F_B(p) = [g_1^T, \cdots, g_m^T]^T. \tag{5}$$

We denote the stacked vector of inter-neighbour bearing measurements as $g = F_B(p)$. Similar to a framework, the *bearing formation*, $(\mathcal{G}, g)$, is defined by mapping the edges in graph $\mathcal{E}$ to the bearing measurements g.

Definition 1. *A bearing vector g is* realizable *with underlying graph $\mathcal{G}$ in $\mathbb{R}^{\mathsf{d}}$, if there exists a configuration $p \in \mathbb{R}^{\mathsf{d}n}$ satisfying all the bearing measurements in g, i.e., $p \in F_B^{-1}(g)$.*

A bearing formation $(\mathcal{G}, g)$ can also be defined directly without any specific configuration p. The key point is to ensure that the bearing vector g is realizable with the graph $\mathcal{G}$.

Recall the example of directed graph as Figure 1b. As shown in Figure 2, a framework $(\mathcal{G}, p)$ in $\mathbb{R}^2$ is constructed by mapping the vertices to the configuration

$$p = \begin{bmatrix} p_1 \\ p_2 \\ p_3 \\ p_4 \end{bmatrix} = \left[\begin{array}{c} 0 \\ 0 \\ \hline 2 \\ 0 \\ \hline 2 \\ -2 \\ \hline 0 \\ -2 \end{array}\right].$$

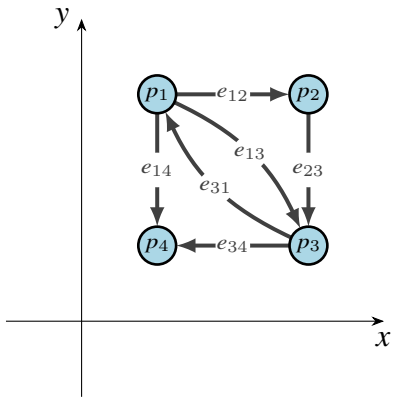

Figure 2: An example of framework with directed underlying graph.

With the framework $(\mathcal{G}, p)$, we can calculate the inter-agent displacement, distance and bearing measurements, such as $z_{12} = p_2 - p_1 = [2, 0]^T, d_{13} = \|p_3 - p_1\| = 2\sqrt{2}, g_{14} = \frac{p_4 - p_1}{\|p_4 - p_1\|} = [0, -1]^T$. In the same way, we can determine the bearing vector:

$$g = \begin{bmatrix} g_{12} \\ g_{23} \\ g_{34} \\ g_{14} \\ g_{13} \\ g_{31} \end{bmatrix} = [(1, 0), (0, -1), (-1, 0), (0, -1), (\sqrt{2}/2, -\sqrt{2}/2), (-\sqrt{2}/2, \sqrt{2}/2)]^T.$$

Then, we call the bearing formation $(\mathcal{G}, g)$ as the corresponding bearing formation of the framework $(\mathcal{G}, p)$. All the inter-neighbour bearing measurements can be found in the bearing vector g. The bearing measurement g_{24} can also be obtained by the framework, and it is an inter-agent bearing measurements.

After introducing the construction of framework, we bring in bearing rigidity theory which further determines the property of the framework.

Theory of Bearing Rigidity.

The rigidity theory focuses on the rigidity or flexibility of a framework. The primary problem that the rigidity theory studies is whether there exists a continuous deformation from a given configuration to another such that edge lengths are preserved. With the distance constrained, it is also called distance rigidity theory. The comprehensive story of distance rigidity theory is presented in the book [35]. In comparison, the bearing rigidity theory studies a similar problem that if there exists a continuous deformation preserving the bearing or direction of edges. In other words, the bearing rigidity theory determines the problem whether a framework can be uniquely determined up to a translation and a scaling factor given the bearings measurement of each edge in the framework.

The theory of bearing rigidity is extensively developed in [11]. Here, we will introduce the main definitions and theorem of bearing rigidity. This problem can

be equivalently stated as whether two frameworks with the same inter-neighbor bearings have the same shape. Consider two frameworks $(\mathcal{G}, p)$ and $(\mathcal{G}, p')$ map the same graph $\mathcal{G}$ to different configurations p and p' in $\mathbb{R}^d$. The notation g_{ij} and g'_{ij} represents the bearing vector between node i and j in frameworks $(\mathcal{G}, p)$ and $(\mathcal{G}, p')$ respectively. These two frameworks are defined to be bearing equivalent if all the inter-neighbour bearing measurements are parallel. Furthermore, if all the inter-agent bearing measurements are parallel, then they are bearing congruent to each other.

Mathematically, we can figure out whether two vectors are parallel with the *orthogonal projection matrix operator*. For any non-zero vector $x \in \mathbb{R}^{\mathsf{d}}\,(\mathsf{d} \geq 2)$, define $P(x) : \mathbb{R}^{\mathsf{d}} \to \mathbb{R}^{\mathsf{d}\times\mathsf{d}}$ as

$$P(x) = I_{\mathsf{d}} - \frac{x}{\|x\|}\frac{x^T}{\|x\|}. \tag{6}$$

For notational simplicity, we denote $P_x = P(x)$. The matrix P_x geometrically projects any vector onto the orthogonal compliment of x. There are some useful properties which can be easily verified such as $P_x^T = P_x$, $P_x^2 = P_x$, $P_x \succcurlyeq 0$ and the most important one,

$$P_x x = 0, \text{or equivalently } \ \mathrm{Null}(P_x) = \mathrm{span}\{x\}. \tag{7}$$

A figure illustrating the geometric properties of the projection matrix is given in Figure 3.

In bearing rigidity theory, the projection matrix is mostly applied to identify whether two bearing vectors are parallel.

Consider two bearing measurement $g, g' \in \mathbb{R}^{\mathsf{d}}\,(\mathsf{d} \geq 2)$. These two bearing vectors are parallel if and only if $P_g g' = 0$.

Then, bearing equivalence and congruence can be mathematically defined with the projection matrix.

Definition 2 ([11]). *The frameworks* $(\mathcal{G}, p)$ *and* $(\mathcal{G}, p')$ *are* bearing equivalent *if* $P_{g_{ij}} g'_{ij} = 0$, *for all* $(i, j) \in \mathcal{E}$.

Definition 3 ([11]). *The frameworks* $(\mathcal{G}, p)$ *and* $(\mathcal{G}, p')$ *are* bearing congruent *if* $P_{g_{ij}} g'_{ij} = 0$, *for all* $i, j \in \mathcal{V}$.

The bearing congruent frameworks are always bearing equivalent since the condition for bearing equivalence is included in the condition for bearing congruence. The definition of globally bearing rigid follow from these concepts.

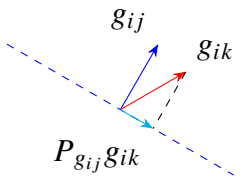

Figure 3: Vector g_{ik} operated by the projection matrix of vector g_{ij}.

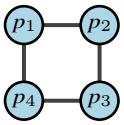

(a) A framework $(\mathcal{G}, p)$.

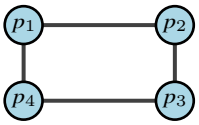

(b) A framework bearing equivalent to $(\mathcal{G}, p)$ in 4a.

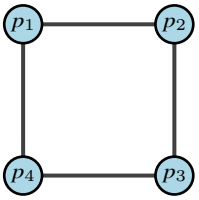

(c) A framework bearing congruent to $(\mathcal{G}, p)$ in 4a.

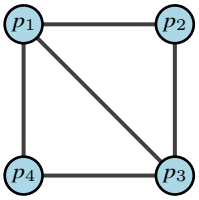

(d) A globally bearing rigid framework.

Figure 4: Frameworks for illustrating globally bearing rigidity.

Definition 4 ([11]). *The framework* $(\mathcal{G}, p)$ *is* globally bearing rigid *(GBR) if an arbitrary framework which is bearing equivalent to* $(\mathcal{G}, p)$ *is bearing congruent to* $(\mathcal{G}, p)$.

In other words, if the framework is globally bearing rigid, any continuous deformation preserving the inter-neighbour bearing will not alter any inter-agent bearing.

Consider the framework 4a, both framework 4b and framework 4c are bearing equivalent to it, but only framework 4c is bearing congruent. It can be concluded that framework 4a is not globally bearing rigid, since there exists a bearing equivalent but not bearing congruent framework 4b.

For a better knowledge of the bearing rigidity theory, we aim to work out the continuous deformation preserving the inter-neighbour bearing measurement, which is the primary problem of rigidity theory. Recall that the bearing vector of inter-neighbour bearing measurement g for the framework $(\mathcal{G}, \mathrm{p})$ can be obtained by the bearing function $\mathrm{g} = F_B(\mathrm{p})$. Let δp be a variation of the configuration p, we are interested in a deformation of the framework by δp such that the bearing vector remains constant to first order. That is, we are looking for vectors δp such that

$$F_B(\mathrm{p} + \delta p) \approx F_B(\mathrm{p}) = \mathrm{g}.$$

We denote such variations as the *infinitesimal bearing motions*.

In this direction, consider the Taylor series expansion of the bearing function F_B at p with small perturbation δp,

$$F_B(\mathrm{p} + \delta p) = F_B(\mathrm{p}) + \frac{\partial F_B}{\partial p}\delta p + \text{h.o.t.}.$$

The higher order terms can be neglected since δp is small. It can be observed that the bearing vector g is maintained, therefore, if

$$\frac{\partial F_B}{\partial p}\delta p = 0.$$

Thus, the Jacobian of the bearing function $\frac{\partial F_B}{\partial p}$ plays an important role, and we define it as the *bearing rigidity matrix* $R_B = \frac{\partial F_B}{\partial p} \in \mathbb{R}^{\mathsf{d}m \times \mathsf{d}n}$. The bearing rigidity matrix can be expressed explicitly by the projection matrix of bearing measurement P_g, the distance measurement d and the extended incidence matrix $\tilde{H} = H \otimes I_{\mathsf{d}}$ as

$$R_B(p) = \operatorname{diag}\left(\frac{P_g}{d}\right)\tilde{H}, \tag{8}$$

where $\operatorname{diag}\left(\frac{P_g}{d}\right) = \operatorname{diag}\left(\frac{P_{g_1}}{d_1}, \frac{P_{g_2}}{d_2}, \cdots, \frac{P_{g_m}}{d_m}\right)$.

The infinitesimal bearing motion can be determined by the null space of bearing rigidity matrix.

Corollary 1. *The dimension of* $\operatorname{Null}(R_B)$ *is at least* $n+1$ *and* $\operatorname{span}\{\mathbb{1}_n \otimes I_{\mathsf{d}}, p\} \subseteq \operatorname{Null}(R_B)$.

Proof. It has be shown before that $H\mathbb{1}_n = 0$ and $P_{g_k} g_k = 0$, which implies that $\tilde{H}(\mathbb{1}_n \otimes I_{\mathsf{d}}) = 0$ and $\operatorname{diag}\left(\frac{P_g}{d}\right)\tilde{H}p = \operatorname{diag}(P_g)g = 0$. Thus, it is sufficient conclude that $\operatorname{span}\{\mathbb{1}_n \otimes I_{\mathsf{d}}, p\} \subseteq \operatorname{Null}(R_B)$. □

Consider the infinitesimal bearing motion $\delta p \in \operatorname{span}\{\mathbb{1}_n \otimes I_{\mathsf{d}}\}$. Every agent shares the same position variation (i.e., $\delta p_i = \delta p_j, \forall v_i, v_j \in \mathcal{V}$). Thus, the variation in space $\operatorname{span}\{\mathbb{1}_n \otimes I_{\mathsf{d}}\}$ is called the motion of translation. In the similar manner, the infinitesimal bearing motion $\delta_p \in \operatorname{span}\{p\}$ is classified as motion of scaling since the deformed framework $(\mathcal{G}, p + \delta p)$ can be seemed as an enlargement or diminution of the origin framework. The translations and scaling infinitesimal motions are called the *trivial* infinitesimal bearing motions.

Definition 5 ([11])**.** *A framework is* infinitesimally bearing rigid *(IBR) if all the infinitesimal bearing motions of the framework are trivial.*

It has been showed that the infinitesimally bearing rigidity always implies globally bearing rigidity [11, Theorem 5]. Moreover, the infinitesimally or globally bearing rigidity of framework $(\mathcal{G}, p)$ also indicates the infinitesimally or globally bearing rigidity of formation $(\mathcal{G}, g)$ generated from $g = F_B(p)$.

In Figure 5, we give two examples of frameworks (vertices and edges) with 4 nodes and their infinitesimal bearing motions (arrows). These two frameworks are related to the same configuration p in $\mathbb{R}^2$, while the underlying graphs are different. The motions corresponding to red and blue arrows are translation and scaling motion, which are the trivial infinitesimal bearing motions. The motions expressed with orange arrows are non-trivial infinitesimal bearing motions. The bearing formation 5a is not infinitesimal bearing rigid since non-trivial motion exists. The bearing formation 5b is infinitesimal bearing rigid since all the infinitesimal bearing motions are trivial. With the following theorem, the property of infinitesimally bearing rigidity is attached to the property of bearing rigidity matrix R_B.

(a) A not infinitesimally bearing rigid framework.

(b) An infinitesimally bearing rigid framework.

Figure 5: Illustrating examples for infinitesimal bearing motion and infinitesimally bearing rigidity.

Theorem 1 ([11]). *For any undirected framework* $(\mathcal{G}, p)$*, the following statements are equivalent:*

i) $(\mathcal{G}, p)$ *is infinitesimally bearing rigid;*

ii) $(\mathcal{G}, p)$ *can be uniquely determined up to a translation and a scaling factor by the inter-neighbor bearings;*

iii) $\mathrm{Rank}(R_B) = \mathsf{d}n - \mathsf{d} - 1$*;*

iv) $\mathrm{Null}(R_B) = \mathrm{span}\{\mathbb{1} \otimes I_{\mathsf{d}}, p\}$.

The statement (iv) indicates the statement (i) and (ii) directly according to the previous introduction. With the dimension of $\mathrm{Null}(R_B)$ equalling to $\mathsf{d}+1$, the rank of R_B should be $\mathsf{d}n - \mathsf{d} - 1$.

Until now we demonstrated that bearing rigidity is a property of framework. In the following we aim to show that the bearing rigidity of a framework is a generic property which is critically determined by the underlying graph rather than the configuration.

Definition 6 ([32]). *A graph* $\mathcal{G}$ *is* generically bearing rigid *(GBR) in* $\mathbb{R}^{\mathsf{d}}$*, if there exists at least one configuration* p *in* $\mathbb{R}^{\mathsf{d}}$ *such that* $(\mathcal{G}, p)$ *is bearing rigid.*

From the definition, if a graph is not generically bearing rigid, there does not exist any configuration such that the framework is bearing rigid. On the other hand, generically bearing rigid graphs possess the following property.

Lemma 1 ([32]). *If* $\mathcal{G}$ *is generically bearing rigid in* $\mathbb{R}^{\mathsf{d}}$*, then* $(\mathcal{G}, p)$ *is global bearing rigid for almost all configuration* p *in* $\mathbb{R}^{\mathsf{d}}$*, in the sense that the set of* p *where* $(\mathcal{G}, p)$ *is not bearing rigid is of measure zero.*

Here, some examples of frameworks in $\mathbb{R}^2$ are given to illustrate the generically bearing rigidity. The underlying graph for Figure 6a is not generically bearing rigid. Thus, there exists no mapping in $\mathbb{R}^2$ leading to a global bearing rigid framework. The underlying graph $\mathcal{G}$ for Figure 6b and 6c is the same. This graph is generically bearing rigid in $\mathbb{R}^2$ since framework 6b is bearing rigid. For almost all the configuration p in $\mathbb{R}^2$, the framework $(\mathcal{G}, p)$ should be bearing rigid, while the framework 6c shows the special case which belongs to a set of measure zero.

A generically bearing rigid graph is essential to form a globally bearing rigid framework. In this section, we will present the definition of the Laman Graphs and Henneberg construction which helps to construct the generically bearing rigid graphs.

Definition 7 ([32]). *A graph $\mathcal{G} = (\mathcal{V}, \mathcal{E})$ is* Laman *if $|\mathcal{E}| = 2|\mathcal{V}| - 3$ and every subgraph with $k > 2$ vertices spans at most $2k - 3$ edges.*

Theorem 2 ([32]). *A graph $\mathcal{G}$ is generically bearing rigid if and only if the graph contains a Laman spanning graph.*

A Laman graph with four vertices is given as Figure 7a. The graph 7b is composed of a Laman graph and an additional edge. Both graph 7a and graph 7a are generically bearing rigid. It is generally difficult to tell whether a graph is Laman or not from the definition as it is a combinatorial property. Thus, the Henneberg construction [32] is introduced as a way to build Laman graphs.

Definition 8. *The Henneberg construction starts from the most elemental Laman graph with a pair of vertices v_1 and v_2 and an edge (v_1, v_2). The graph $\mathcal{G} = (\mathcal{V}, \mathcal{E})$ can be enlarged by performing one of the following two operations:*

1) Vertex addition*: connect a new vertex v_i to $\mathcal{G}$ to any two existing vertices $v_j, v_k \in \mathcal{V}$. The extended graph $\mathcal{G}'$ can be expressed by $\mathcal{V}' = \mathcal{V} \bigcup \{v_i\}$ and $\mathcal{E}' = \mathcal{E} \bigcup \{e_{ij}, e_{ik}\}$.*

2) Edge splitting*: Suppose three vertices $v_j, v_k, v_l \in \mathcal{V}$ and $e_{jk} \in \mathcal{E}$. A new vertex v_i can be connected to v_j, v_k, v_l by deleting edge e_{jk}. The extended graph $\mathcal{G}'$ can be expressed by $\mathcal{V}' = \mathcal{V} \bigcup \{v_i\}$ and $\mathcal{E}' = \mathcal{E} \bigcup \{e_{ij}, e_{ik}, e_{il}\} \setminus \{e_{jk}\}$.*

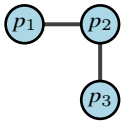

(a) A Framework that is not bearing rigid.

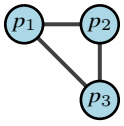

(b) A bearing rigid framework indicates its underlying graph is generically bearing rigid.

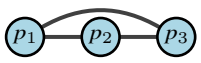

(c) A generically bearing rigid graph in a non-generic position leads to a not bearing rigid framework.

Figure 6: Illustrating frameworks for generically bearing rigidity.

(a) A Laman graph. (b) A graph containing a Laman graph.

Figure 7: Illustrating examples of Laman graphs.

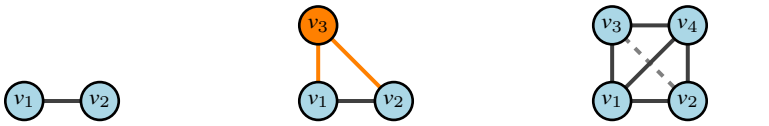

(a) Starting graph. (b) Vertex addition. (c) Edge splitting.

Figure 8: Illustrating examples for Henneberg construction.

The graph built with Henneberg construction is always a Laman graph. Associated with Theorem 2, any graph $\mathcal{G}$ built by adding edges to a graph with Henneberg construction is generically bearing rigid in $\mathbb{R}^d$, which leads the framework $(\mathcal{G}, p)$ to be bearing rigid for almost all configuration $p \in \mathbb{R}^d$.

Figure 8 exhibits the procedure of Henneberg construction. It starts with two vertices and an edge between them. The node v_3 is added by vertex addition and the node v_4 is appended by edge splitting with deleting e_{23}. The graph can continue to be enlarged by repeating these two operations.

The introduction of bearing rigidity theory is completed so far. As a conclusion, the bearing rigidity theory shows the requirement to uniquely define a structure or the shape of a framework by bearing constraints.

2.2 Bearing-Only Formation Control on Undirected Graphs

Formation control is a concept rooted in multi-agent system and control theory, focusing on guiding multiple agents to achieve and maintain a desired geometric pattern. In bearing formation control, the geometric pattern is based on bearing measurements. The bearing-only formation control (BOFC) law was firstly proposed in [11]. In this section, we will mathematically formulate the bearing formation control problem and then demonstrate how the bearing-only formation control law solves the problem.

Problem Formulation. The bearing formation control problem is to design a distributed control protocol which drives a multi-agent system to some desired condition. Firstly, we use a graph $\mathcal{G} = (\mathcal{V}, \mathcal{E})$ called the sensing graph to describe sensing or the capability of communication between agents in the MAS. We focus on the undirected sensing graph in this section, implying that the communication between two agents are symmetric, i.e., if $e_{ij} \in \mathcal{E}$ then $e_{ji} \in \mathcal{E}$. The agents are modeled using single integrator dynamics,

$$\dot{p}_i = u_i,\ i = 1, \ldots, n, \tag{9}$$

where $u_i \in \mathbb{R}^{\mathrm{d}}$ is the control. The target geometric pattern for the bearing formation control problem is specified by a target bearing formation $(\mathcal{G}, \mathrm{g})$. The underlying graph of the target bearing formation should be identical to the sensing graph of the MAS. The target bearing vector g should also satisfy a feasibility condition, as shown in the following assumption.

Assumption 1. *For the target bearing formation* $(\mathcal{G}, \mathrm{g})$*, there exists an infinitesimally bearing rigid framework* $(\mathcal{G}, \mathrm{p})$ *satisfying all the bearing measurement in* g *(i.e.,* $\mathrm{g}_{ij} = \frac{\mathrm{p}_j - \mathrm{p}_i}{\|\mathrm{p}_j - \mathrm{p}_i\|}, \forall e_{ij} \in \mathcal{E}$*).*

Actually, the feasibility assumption can be comprehended as: *i*) the sensing graph $\mathcal{G}$ is generically bearing rigid; *ii*) the target bearing vector g is not in the set of measure zero leading to the non-bearing rigid frameworks; *iii*) the bearing vector g is realizable.

Another common assumption relates to collisions.

Assumption 2. *There are no collisions of agents along trajectories of the system.*

Then, the general bearing formation control problem can be stated formally.

Problem 1. *Given a target bearing formation* $(\mathcal{G}, \mathrm{g})$ *satisfying Assumption 1 and the initial framework* $(\mathcal{G}, p(t_0))$*, design a control law for each agent* $i \in \mathcal{V}$ *modelled by* (9) *based on the inter-neighbour bearing measurements* $\{g_{ij}(t)\}_{(i,j)\in\mathcal{E}}$*, such that*

$$\lim_{t\to\infty} g(t) = \lim_{t\to\infty} F_B(p(t)) = \mathrm{g}.$$

In this paragraph, we will clarify the notation in bearing formation control. The set of current measurements is denoted by the italic letters, as z, d, g, p, representing the current displacement vector, distance vector, bearing vector, and configuration. The set of target bearing vectors is denoted by the regular letter g, while the measurement related to the target bearing formation is also denoted by regular letters such as $\mathrm{z}, \mathrm{d}, \mathrm{p}$.

The Bearing-only Formation Control Law. In this section we consider a solution to Problem 1 for undirected sensing graphs initially proposed in [11]. The nonlinear bearing-only control law is given as

$$u_i = -\sum_{j\in\mathcal{N}_i} P_{g_{ij}} \mathrm{g}_{ij}, \forall i \in \mathcal{V}. \tag{10}$$

It can be also expressed in matrix form as

$$u = \tilde{H}^T \operatorname{diag}(P_g)\mathrm{g}, \tag{11}$$

where $\tilde{H} = H \otimes I_{\mathrm{d}}$ and $\operatorname{diag}(P_g) = \operatorname{diag}(P_{g_1}, P_{g_2}, \cdots, P_{g_m})$.

Theorem 3 ([11])**.** *The bearing-only formation control law* (10) *drives the MAS to a final configuration* p *satisfying the target formation* $(\mathcal{G}, \mathrm{g})$ *(i.e.,* $F_B(\mathrm{p}) = \mathrm{g}$*) exponentially fast from almost any initial configurations* $p(t_0)$*.*

There exist two realizable bearing vectors satisfying the equilibrium condition $\dot{p} = u = \tilde{H}^T \operatorname{diag}(P_g)\mathrm{g} = 0$, which are g and $-\mathrm{g}$. The equilibrium g coincides with the target formation $(\mathcal{G}, \mathrm{g})$ is called the desired equilibrium and the other equilibrium $-\mathrm{g}$ is called the undesired equilibrium. The stability can be verified by the Lyapunov function $V = \frac{1}{2}\|g - g^*\|^2$. The result shows that the desired equilibrium is almost globally exponentially stable and the undesired equilibrium is unstable. The 'almost' refers to the entire state-space except the single unstable equilibrium point.

Example 1. *In Figure 9, an example of simulation is displayed to show how BOFC works and drives the agents to the desired bearing formation. In this example, the target bearing formation is a square in* $\mathbb{R}^2$ *as shown in 9a. The sensing graph*

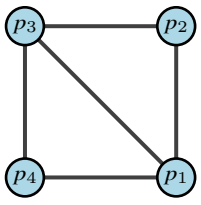

(a) The target formation

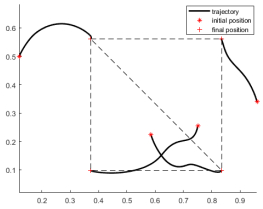

(b) Trajectory: Exerting BOFC on the undirected sensing graph.

Figure 9: A simulation example showing the performance of BOFC.

of MAS is the same as the underlying graph, which is generically bearing rigid. We set the initial position of each agent to be random. The random data taken in this simulation is $p_1(t_0) = [0.1190, 0.4984]^T$, $p_2(t_0) = [0.9597, 0.3404]^T$, $p_3(t_0) = [0.5853, 0.2238]^T$, $p_4(t_0) = [0.7513, 0.2551]^T$. *From the simulated trajectory, it can be found that the system is brought to a final formation as desired.*

2.3 Bearing-Only Formation Control with Directed Sensing

In last section, we introduced the bearing-only formation control law (11) and showed that this control law solves the bearing formation control problem (Problem 1) for undirected sensing graphs. In this section, we are going to introduce the BOFC for MAS with directed graphs, based on the work [29].

Problem Formulation.

Compared with the bearing formation control problem stated in last section, the main change is that the sensing condition is described by a directed graph $\mathcal{G}(\mathcal{V}, \mathcal{E})$. That is, $e_{ij} \in \mathcal{E}$ does not imply that $e_{ji} \in \mathcal{E}$, and sensing is not symmetric.

The target formation $(\mathcal{G}, \mathrm{g})$ is defined after the directed sensing graph $\mathcal{G}$. To ensure that the shape of the target formation can be uniquely determined, the target bearing vector g should satisfy the assumption 1.

Other than the sensing graph and target formation, the system is formulated in the same way including the assumptions. The bearing formation control problem with directed sensing is stated as following:

Problem 2. *Given a target bearing formation* $(\mathcal{G}, \mathrm{g})$ *over a directed graph* $\mathcal{G}$ *satisfying Assumption 1 and the initial framework* $(\mathcal{G}, p(t_0))$*, design a control law for each agent* $i \in \mathcal{V}$ *modelled by* (9) *based on the inter-neighbour bearing measurements* $\{g_{ij}(t)\}_{(i,j)\in\mathcal{E}}$*, such that*

$$\lim_{t\to\infty} g(t) = \lim_{t\to\infty} F_B(p(t)) = \mathrm{g}.$$

It has demonstrated that the bearing-only formation control (10) is a solution to the bearing formation control problem with undirected sensing (Problem 1). In this section, we want to slightly modify the controller to fit the directed sensing condition and find the difference between control systems.

The bearing-only formation control law with directed sensing can be expressed as

$$u_i = -\sum_{j\in\mathcal{N}_i} P_{g_{ij}} \mathrm{g}_{ij}, \forall i \in \mathcal{V}. \tag{12}$$

The directed sensing graph implies that $v_i \in \mathcal{N}_j$ and $v_j \in \mathcal{N}_i$ may not hold simultaneously. Thus, the matrix form should be modified as

$$u = -\tilde{H}_{out}^T \,\mathrm{diag}(P_g)\mathrm{g}, \tag{13}$$

where $\tilde{H}_{out} = H_{out} \otimes I_{\mathsf{d}}$.

The directed sensing brings asymmetry to the control system, which may change the convergence of the system. Thus, it can not be determined whether the bearing-only formation control with directed sensing (12) is the solution to the bearing formation control problem with directed sensing condition (problem 2).

The main contribution of [29] was presenting that for a certain class of directed graphs, the control (13) can solve the directed BOFC problem. In the sequel we review the structure of this class of graphs.

Leader-First-Follower Graphs.

In [29], it was shown that the MAS can be asymptotically driven to the target formation if the sensing graph belongs to a special class of graph called the *leader first-follower graph generated from a bearing-based Henneberg construction (HCLFF)*. The Henneberg construction for undirected graphs were defined in the Section 2.1. The operation of construction for directed graphs is quite similar to the undirected graphs.

Definition 9. *The* directed Henneberg construction *of directed graph starts from a pair of vertices v_1 and v_2 and a directed edge e_{21}. The graph $\mathcal{G} = (\mathcal{V}, \mathcal{E})$ can be enlarged by performing one of the following two operations:*

1) Vertex addition*: connect a new vertex v_i to $\mathcal{G}$ to any two existing vertices $v_j, v_k \in \mathcal{V}$. The extended graph $\mathcal{G}'$ can be expressed by $\mathcal{V}' = \mathcal{V} \bigcup \{v_i\}$ and $\mathcal{E}' = \mathcal{E} \bigcup \{e_{ij}, e_{ik}\}$.*

2) Edge splitting*: Suppose three vertices $v_j, v_k, v_l \in \mathcal{V}$ and $e_{jk} \in \mathcal{E}$. A new vertex v_i can be connected to v_j, v_k, v_l by deleting edge e_{jk}. The extended graph $\mathcal{G}'$ can be expressed by $\mathcal{V}' = \mathcal{V} \bigcup \{v_i\}$ and $\mathcal{E}' = \mathcal{E} \bigcup \{e_{ji}, e_{ik}, e_{il}\} \setminus \{e_{jk}\}$.*

Figure 10 shows the procedure to construct a directed graph by Henneberg construction. Then, in Figure 11, the difference between the undirected graph and directed graph generated from Henneberg construction can be identified.

The Henneberg construction can now be used to build the so-called leader-first-follower graphs generated from Henneberg construction, which is defined as following.

Definition 10 (LFF Graphs)**.** *A directed graph is a* leader-first-follower graph generated from Henneberg construction *(HCLFF graph) if*

i) there is a vertex with no outgoing edges, denoted as the leader*, assigned the label v_1;*

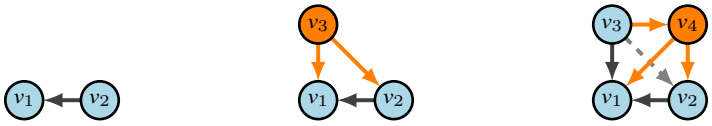

(a) Starting graph. (b) Vertex addition. (c) Edge splitting.

Figure 10: Illustrating examples for Henneberg construction of directed graphs.

(a) An undirected graph generated from Henneberg construction.

(b) A directed graph generated from Henneberg construction.

Figure 11: Illustrating examples for Henneberg construction.

ii) *there is a vertex with only one outgoing edge pointing to the leader, denoted as the* first follower *assigned the label* v_2*;*

iii) *every vertex other than the leader and first follower has exactly two outgoing edges;*

iv) *for every directed edge* e_{ij}*, the label* $i > j$*.*

From the condition (*iv*) of Definition 10, all the edge starts from an vertex with larger label and points to a vertex with smaller label. Based on which, we define the following notation.

Definition 11. *For a directed edge* e_{ij}*, if* $i < j$*, it is denoted as a* backward edge*. If* $i > j$*, it is denoted as a* forward edge*.*

In other words, all the edges in the HCLFF graph are forward edges. Thus, we regard that the structure is ordered, which is the main property of HCLFF graph.

Figure 12 is given to shown the orderliness of the HCLFF graph. It can be verified that all the edges are in the same direction (from right to left).

Recall that in Section 2.1 we introduced that the Henneberg construction helps to generate the Laman graph, which ensures the generic bearing rigidity of the graph. This property also holds for the directed construction [29] for the directed graphs too. For a target bearing formation $(\mathcal{G}, \mathrm{g})$, whose underlying graph is a HCLFF

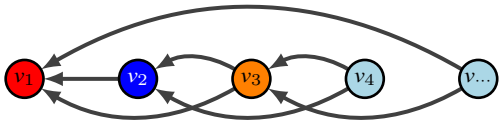

Figure 12: An example of a HCLFF graph.

graph, the bearing formation $(\mathcal{G}, \mathrm{g})$ is IBR if the attached target bearing vector g is not in a special set of measure zero. Particularly for the HCLFF graph, the bearing vector g is not in the set of measure zero if the outgoing edges of each agent are not parallel. Furthermore, the target configuration satisfying the IBR target formation can be uniquely defined if the underlying graph is HCLFF graph.

Lemma 2 ([29]). *If the graph $\mathcal{G}$ is HCLFF, then the target framework $(\mathcal{G}, \mathrm{p})$ satisfying the IBR target formation $(\mathcal{G}, \mathrm{g})$ can be uniquely determined by the leader's position $p_1(t_0)$ and the distance between the leader and first follower $d_{21}(t_0)$. More specifically, the target position for each agent can be calculated using the following set of equations (in order),*

$$\begin{aligned}
\mathrm{p}_1 &= p_1(t_0) \\
\mathrm{p}_2 &= \mathrm{p}_1 - d_{21}(t_0)\mathrm{g}_{21} \\
\mathrm{p}_i &= \left(\sum_{j\in\mathcal{N}_i} P_{\mathrm{g}_{ij}}\right)^{-1}\left(\sum_{j\in\mathcal{N}_i} P_{\mathrm{g}_{ij}}\mathrm{p}_j\right), \ \textit{for } i = 3, \cdots, n.
\end{aligned}$$

As an explanation, the initial position of the leader and the initial distance between the leader and first follower determines the translation and scale of the target framework. Once the target position for the leader and first follower is determined, the target position for the other agents can be geometrically obtained by their two outgoing edges.

The Bearing-Only Control Law for Directed Sensing.

Previously, the bearing-only formation control with directed sensing is well defined as (13). We have also displayed the definition and property of the HCLFF graph. In the work [29], they investigated how the bearing-only formation control works with the HCLFF graph as the directed sensing.

The main property of the HCLFF graph is the orderliness. It implies that all the outgoing edges of agent v_i point to the agents with smaller label. In other words, the agent v_i can only acquire the bearing measurement relative to the agents with label smaller than i.

Consequently, the complete bearing-only formation control system can be written as

$$\begin{bmatrix} \dot{p}_1 \\ \dot{p}_2 \\ \dot{p}_3 \\ \vdots \\ \dot{p}_n \end{bmatrix} = \begin{bmatrix} u_1(p_1) \\ u_2(p_1, p_2) \\ u_3(p_1, p_2, p_3) \\ \vdots \\ u_n(p_1, p_2, p_3, \cdots, p_{n-1}, p_n) \end{bmatrix}. \tag{14}$$

Here, $u_i = -\sum_{j\in\mathcal{N}_i} P_{g_{ij}} \mathrm{g}_{ij}$ is the control for each agent. In Appendix A, the stability theory of cascade systems is introduced in detail. Obviously, the triangular structure appears in (14). By the stability theory of cascade system, we are able to decompose the system and perform the equilibrium and stability analysis one equation at a time.

The convergence of the nonlinear cascade system (14) is given in [29, Thm. 1].

Theorem 4 ([29])**.** *For a multi-agent system on a HCLFF graph, the bearing-only formation control law (12) asymptotically drives the MAS to the target configuration* p *determined by the IBR target formation* $(\mathcal{G}, \mathrm{g})$ *from almost any initial configuration* $p(t_0)$*.*

We will briefly explain the proof of Theorem 4 in the following paragraphs. The investigation of the cascade system (14) starts with the leader and first follower. The leader stays at its initial position, which is also the target position $p_1^* = \mathrm{p}_1 = p_1(t_0)$. The distance between the leader and first follower d_{21} is invariant. The first follower moves in a trajectory of a circle with p_1 as the center. Two equilibrium $p_{2a}^* = p_1^* - d_{21}\mathrm{g}_{21}$ and $p_{2b}^* = p_1^* + d_{21}\mathrm{g}_{21}$ exists.

For the agents other than LFF, they have exactly two outgoing edges. Consider agent v_3 as an example. The relevant dynamic equation is

$$\dot{p}_3 = -P_{g_{31}}\mathrm{g}_{31} - P_{g_{32}}\mathrm{g}_{32}.$$

The equilibrium of p_3 is a function of p_1 and p_2, which takes the form as

$$p_3 = \left(P_{g_{31}} + P_{g_{32}}\right)^{-1}\left(P_{g_{31}}p_1 + P_{g_{32}}p_2\right).$$

From the previous analysis, we find two groups of equilibrium for LFF. Therefore, agent v_3 has two equilibrium p_{3a}^* and p_{3b}^* corresponding to (p_1^*, p_{2a}^*) and (p_1^*, p_{2b}^*) separately.

By induction, the other agents are analyzed in the same way as agent v_3. The whole system has two sets of equilibrium stated as p_a^* and p_b^*. The equilibrium p_a^* is exactly the unique configuration satisfying the target formation ($p_a^* = \mathrm{p}$) and p_b^* is symmetric to p_a^* with respect to p_1^*.

Figure 13 concisely demonstrates the relation between the two equilibrium. In the work [29], the stability of equilibrium is proved by the stability theorem of cascade structure. The desired equilibrium p_a^* is an almost globally asymptotically stable equilibrium, while the other equilibrium p_b^* is unstable.

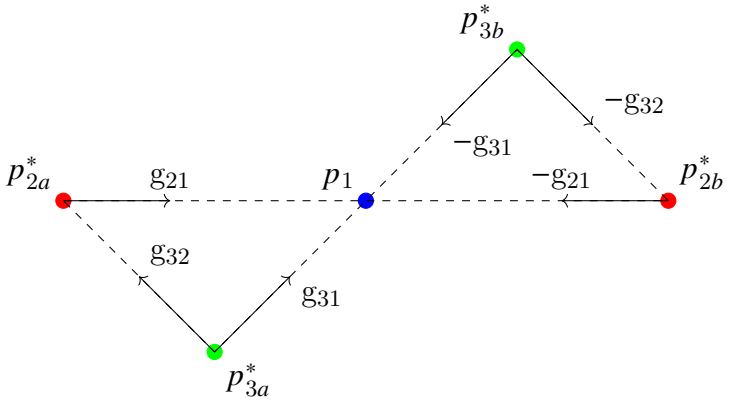

Figure 13: Illustration graph for the equilibrium p^*_a and p^*_b.

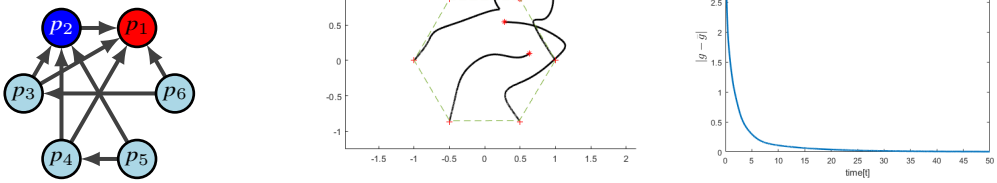

(a) The target bearing formation.

(b) System trajectories.

(c) Bearing error along the system trajectories.

Figure 14: Simulation: Exerting BOFC on the MAS with target bearing formation in LFF formation generated from Henneberg construction.

Example 2. *Figure 14a shows the target formation, which is an LFF formation generated from the directed Henneberg construction. In Figure 14b, it can be found that the leader v_1 stays at the initial condition and the first follower v_2 moves as an arc. All the other agents converges to the final configuration satisfying the target bearing formation. Figure 14c shows that the error between the target bearing vector and the current bearing vector asymptotically converges to zero.*

3 Bearing Formation Control with Extended LFF Graphs

As we introduced in the previous chapter, the BOFC on directed graphs was studied in [29]. The directed graph they analyzed is the LFF structure generated from Henneberg construction. With such directed graph and appropriate target bearing measurement (satisfying Assumption 1), the bearing-only formation control protocol is able to bring the MAS to the target formation from almost any initial condition. In this research, we are interested in expanding a more general condition on the directed sensing graph such that the MAS still converges to the target formation.

3.1 Problem Motivation

In this section, we aim to motivate the expansion on the condition of directed sensing along with some illustrative numerical simulations. The graph to be generalized is the HCLFF graph. In Definition 10, we required four properties for the HCLFF graph, indicating that HCLFF just represents a restrictive class of directed graphs. There are many directed graphs not satisfying the properties of HCLFF graph. We are interested if the formation control problem can still be solved with more general graphs.

Example 3. *Consider the target formation in Figure 15a. Observe that the underlying graph is not a HCLFF graph since some of the follower nodes have more than two outgoing edges. On the other hand, all the edges in light blue show a subgraph that is a HCLFF graph. The trajectories of the BOFC system* (13) *with this sensing graph are shown in Figure 15b. It can be seen that the agents converge to the desired formation shape and the bearing error converge to the zero, indicating that this sensing graph structure can still solve the formation control problem.*

Example 4. *Consider the target formation in Figure 16a. Observe that the underlying graph is an extension of the HCLFF graph with all the edges in light blue*

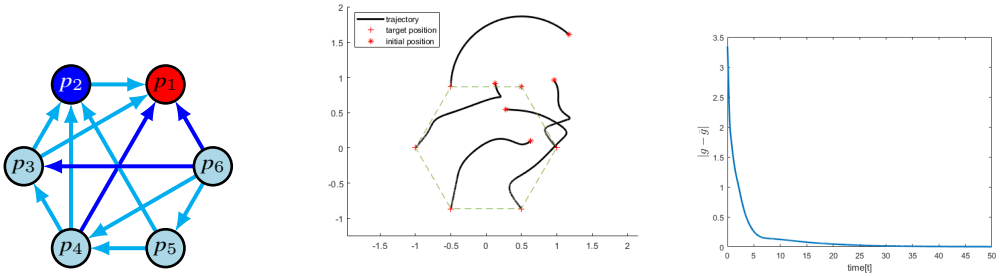

(a) The target formation. (b) Trajectory of BOFC with directed target formation as 15a. (c) Bearing error along the system trajectories.

Figure 15: The first trial of graph expansion.

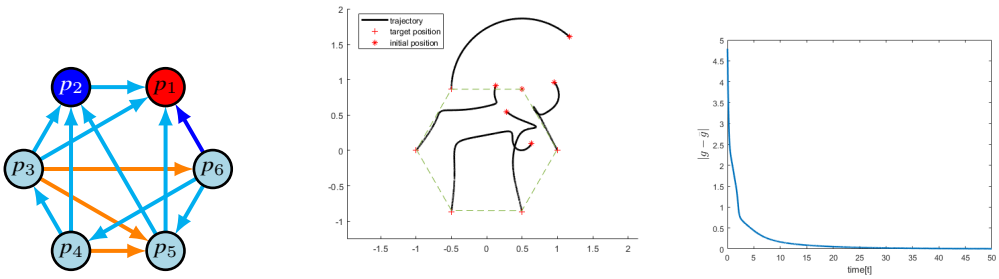

(a) The target formation. (b) Trajectory of BOFC with directed target formation as 16a. (c) Bearing error along the system trajectories.

Figure 16: The second trial of graph expansion.

showing a subgraph that is a HCLFF graph. Nonetheless, with extra forward edges (blue edges) and backward edges (orange edges) included in this graph, the orderliness in the graph is broken and there exists more than two outgoing edges for the agents. The trajectories of the BOFC system (13) *with this sensing graph are shown in Figure 16b. It can be seen that the agents converge to the desired formation shape and the bearing error converge to the zero, indicating that this sensing graph structure can still solve the formation control problem.*

Example 5. *Consider the target formation in Figure 17a. Its underlying graphs contains a leader and a first follower and the HCLFF graph is not contained as a subgraph. The trajectory of the BOFC* (13) *with such target formation is shown in Figure 17b. We can conclude that the BOFC* (13) *does not drive the system to the target formation. From Figure 17c, it can be found the bearing error actually converges to zero. The main reason is that this target formation does not meet the requirement of bearing rigidity.*

Example 6. *Consider the target formation in Figure 18a. The underlying graphs*

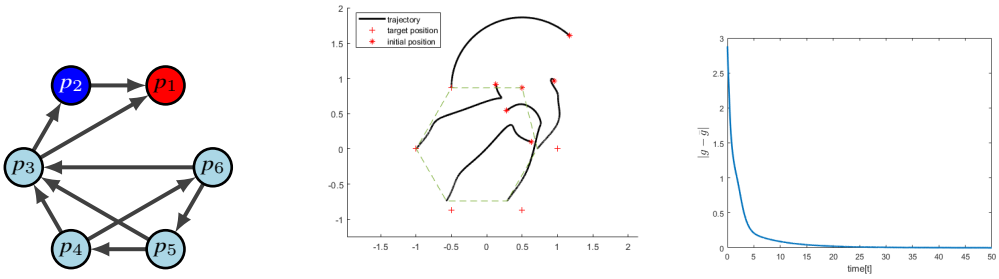

(a) The target formation. (b) Trajectory of BOFC with directed target formation as 17a. (c) Bearing error along the system trajectories.

Figure 17: The third trial of graph expansion.

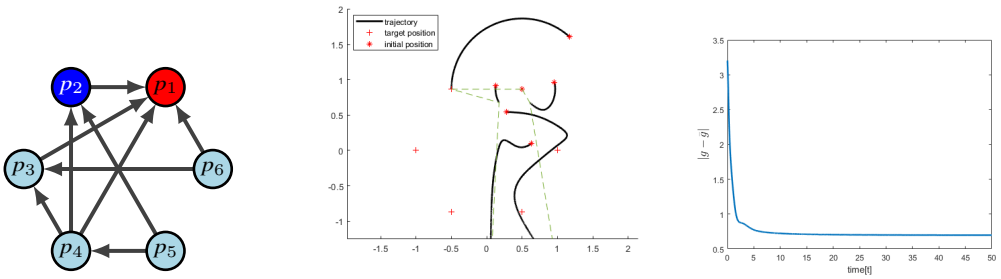

(a) The target formation. (b) Trajectory of BOFC with directed target formation as 18a. (c) Bearing error along the system trajectories.

Figure 18: The forth trial of graph expansion.

contains a leader and a first follower. However, the HCLFF graph can not be found as a subgraph. The trajectory of the BOFC (13) *with this sensing graph and the bearing error along the trajectory are shown in Figure 18b and Figure 18c. We can conclude that the BOFC* (13) *does not solve the formation control problem (Problem 2) with such sensing graph.*

3.2 Formulation of Principle Problem

The principle problem investigated in this research is now presented. The multi-agent control system is built with arbitrary number of agents. The sensing condition of the system is directed and been described by a directed graph $\mathcal{G} = (\mathcal{V}, \mathcal{E})$. The target formation $(\mathcal{G}, \mathrm{g})$ composed of the sensing graph $\mathcal{G}$ and a target bearing set g should be IBR (satisfy the Assumption 1). The following problem is the main task of the thesis.

Problem 3. *Given a target bearing formation* $(\mathcal{G}, \mathrm{g})$ *over a directed graph* $\mathcal{G}$ *satisfying Assumption 1 and the initial framework* $(\mathcal{G}, p(t_0))$*, determine the condition for the sensing graph* $\mathcal{G}$ *such that the bearing-only formation control law* (13) *drives the system to target formation, i.e.,*

$$\lim_{t\to\infty} g(t) = \lim_{t\to\infty} F_B(p(t)) = \mathrm{g}.$$

3.3 BOFC on System with 1 Follower and Many Leaders (1-to-Many)

One of the most important properties of the LFF formation generated from Henneberg construction is that there are at most two outgoing edges for each agent. In the last section, we presented some idea of graph extension, in which more outgoing edges exist for some agents. Before working on a more general setup, we begin with a single agent with more than two outgoing edges.

In this section, we will define a simple system, in which there is only one agent able to sense other agents during the motion. The rest of agents in the MAS cannot obtain any information of measurements. All the agents in MAS are controlled by bearing-only formation control law, leading that only one agent is moving and other agents are fixed. Thus, we call this system as a one degree of freedom system (1-to-many system). With the equilibrium analysis on the simple system, we aim to find out how the BOFC works on each single agent.

Problem Formulation.

In this section, we will formally define the 1-to-many system. Consider the MAS with $n+1$ agents modeled by a single integrator (9). The first n agents $v_1, \cdots, v_n$ will all be considered as leaders, and consequently do not move in this setting. We denote this vertex set for the leaders as $\mathcal{V}_0 = \{v_1, \cdots, v_n\}$. The last agent which allowed to move is denoted as v_c. The complete control system can be expressed as

$$\begin{aligned} \dot{p}_i &= 0, \forall v_i \in \mathcal{V}_0 \\ \dot{p}_c &= u_c, \end{aligned} \tag{15}$$

where the control of agent c is the bearing-only control used in (12).

The directed sensing graph of the MAS $\mathcal{G} = (\mathcal{V}, \mathcal{E})$ is shown in Figure 19 and consists of $|\mathcal{V}| = |\mathcal{V}_0| + 1 = n + 1$ agents and $|\mathcal{E}| = n$ edges. All n edges start from agent c and point to the n leader agents. Note that $|\mathcal{N}_i| = 0, \forall v_i \in \mathcal{V}_0$ and $\mathcal{N}_c = \mathcal{V}_0$.

After establishing the sensing graph, the next step is to settle the target bearing formation. In the common bearing formation problem (Problem 2), the target bearing vector g satisfies the Assumption 1. We stick with this assumption in the 1-to-many system.

Assumption 3. *For the target bearing formation* $(\mathcal{G}, \mathrm{g})$*, there exists a configuration* p *satisfying all the bearing measurement in* g *(i.e.,* $\mathrm{g}_{ij} = \frac{\mathrm{p}_j - \mathrm{p}_i}{\|\mathrm{p}_j - \mathrm{p}_i\|}, \forall e_{ij} \in \mathcal{E}$*) and* $\mathrm{p}_i, \mathrm{p}_j, \mathrm{p}_c$ *are not collinear for any two agents* $v_i, v_j \in \mathcal{V}_0$*.*

Note that Assumption 3 is different from Assumption 1. In Assumption 3, the configuration satisfying the target formation is assumed to be infinitesimally bearing

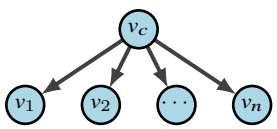

Figure 19: Sensing graph for the 1-to-many control system with $|\mathcal{V}| = n + 1$ agents.

rigid since we hope the shape of target formation can be uniquely defined by the target bearing vector. Here in Assumption 3, the sensing graph of the 1-to-many system is not generically bearing rigid, indicating that there will not be any IBR framework satisfying the target formation. Nonetheless, if $n \geq 2$, the position of the agent v_c can be uniquely defined with the fixed agents.

Moreover, since the leader agents do not move in the 1-to-many system, their final position is determined by their initial condition. Thus, an assumption on the initial condition of the fixed agents should be made according to the target bearing formation.

Assumption 4. *For the initial position of the fixed agents* $\{p_1(t_0), \cdots, p_n(t_0)\}$*, there exists a target position* p_c *for the controlled agent* v_c*, such that the configuration* $p = [p_1(t_0)^T, p_2(t_0)^T, \cdots, p_n(t_0)^T, \mathrm{p}_c^T]^T$ *satisfies all the bearing measurement in the target bearing formation* $(\mathcal{G}, \mathrm{g})$*.*

As discussed before, the target position p_c can be uniquely defined with the Assumption 4.

Lemma 3. *For the 1-to-many system with at least two leaders (i.e.,* $n \geq 2$*), if the target formation* $(\mathcal{G}, \mathrm{g})$ *satisfies Assumption 3 and the initial condition of the fixed agents satisfies Assumption 4, then the target position of the controlled agent* p_c *is*

$$\mathrm{p}_c = \left(\sum_{i=1}^{n} P_{\mathrm{g}_{ci}}\right)^{-1} \left(\sum_{i=1}^{n} P_{\mathrm{g}_{ci}} p_i(t_0)\right).$$

Proof. The target position p_c along with the initial condition of the fixed agents should satisfy the target bearing formation, i.e.,

$$P_{\mathrm{g}_{ci}}(p_i(t_0) - \mathrm{p}_c) = 0, \forall i = 1, \cdots, n \tag{16}$$

From (16), if follows that

$$\sum_{i=1}^{n} P_{\mathrm{g}_{ci}}(p_i(t_0) - \mathrm{p}_c) = 0. \tag{17}$$

It can be simplified as

$$\left(\sum_{i=1}^{n} P_{\mathrm{g}_{ci}}\right) \mathrm{p}_c = \left(\sum_{i=1}^{n} P_{\mathrm{g}_{ci}} p_i(t_0)\right). \tag{18}$$

Consider two non-parallel vectors $x \in \mathbb{R}^{\mathsf{d}}, y \in \mathbb{R}^{\mathsf{d}}$ and their projection matrices P_x, P_y. From the property of projection matrix (7), their kernel space is $\mathrm{Null}(P_x) = \mathrm{span}\{x\}, \mathrm{Null}(P_y) = \mathrm{span}\{y\}$. Since x is not parallel with y, the subspace

$$\mathrm{Null}(P_x) \bigcap \mathrm{Null}(P_y) = \mathrm{span}\{x\} \bigcap \mathrm{span}\{y\} = \{0\}.$$

In addition, the projection matrix is always positive semi-definite. The kernel space of two positive semi-definite matrices is the intersection of the kernel space of these two matrices (i.e., $\text{Null}(P_x + P_y) = \text{Null}(P_x) \bigcap \text{Null}(P_y)$). Thus, the space $\text{Null}(P_x + P_y) = \{0\}$, implying that $P_x + P_y$ is invertible.

As the same reason, the matrix $\left(\sum_{i=1}^{n} P_{\mathrm{g}_{ci}}\right)$ is invertible because $\mathrm{g}_{ci} \neq \mathrm{g}_{cj}, \forall i, j = 1, \ldots, n$ holds with the target bearing vector g satisfying Assumption 3. Followed by equation (18), the target position p_c is obtained as Lemma 3. □

Along with the collision avoidance assumption (Assumption 2), the problem can be formulated as following, which is the main work of this section.

Problem 4. *For the system with one follower and many leaders, given a target bearing formation* $(\mathcal{G}, \mathrm{g})$ *satisfying Assumption 3 and the initial framework* $(\mathcal{G}, p(t_0))$*, determine whether the bearing-only formation control law* (13) *drives the system to target formation, i.e.,*

$$\lim_{t\to\infty} g(t) = \lim_{t\to\infty} F_B(p(t)) = \mathrm{g}.$$

Equilibrium Analysis of System with 1 Follower and Many Leaders.

Apply the bearing-only formation control law (12) on the 1-to-many system (15). The system dynamic can be expressed as

$$\begin{aligned} \dot{p}_i &= 0, \forall v_i \in \mathcal{V}_0 \\ \dot{p}_c &= -\sum_{j=1}^{n} P_{g_{cj}} \mathrm{g}_{cj}. \end{aligned} \tag{19}$$

The number of outgoing edges for agent c, which is also the number of all the edges in $\mathcal{E}$, directly affects the complexity of Problem 4. We can, however, solve the problem for the simpler cases. Note that the case with zero outgoing edge is degenerate. According to the number of agents ($|\mathcal{V}| = n + 1$) or edges ($|\mathcal{E}| = n$), the problem should be separated to two special cases: *i*) $n \leq 2$, and *ii*) $n > 2$. We analyze them below.

Less Than Two Outgoing Edges ($n \leq 2$) The first two cases have already been worked out in [29]. We present the main result from [29] with the proof given in Appendix B.

Lemma 4 ([29])**.** *For the system (19) with* $n = 1$*, the distance* d_{c1} *is invariant during the full motion. There are two equilibrium for the system. The first equilibrium* $p^*_{ca} = p_1 - d_{c1}\mathrm{g}_{c1}$ *is almost globally asymptotically stable. The second one* $p^*_{cb} = p_1 + d_{c1}\mathrm{g}_{c1}$ *is unstable.*

Lemma 5 ([29])**.** *For the system (19) with* $n = 2$*, there is a unique equilibrium point* $p^*_c = (P_{\mathrm{g}_{c1}} + P_{\mathrm{g}_{c2}})^{-1}(P_{\mathrm{g}_{c1}} p_1 + P_{\mathrm{g}_{c2}} p_2)$ *and it is global asymptotically stable.*

More Than Two Outgoing Edges ($n > 2$) Consider the dynamic equation of agent c as shown in (19), from which it can be observed that the control protocol is expressed explicitly by the current bearing g and target bearing g,

$$\dot{p}_c = u_c(g, \mathrm{g}) = -\sum_{j=1}^{n} P_{g_{cj}} \mathrm{g}_{cj}. \tag{20}$$

In the formation control problem, the target bearing vector g satisfying Assumption 3 is primarily defined. The equilibrium analysis aims to find the bearing vector g satisfying the equilibrium condition $\dot{p}_c = u_c(g, \mathrm{g}) = 0$ according to the target bearing g. Meanwhile, as a bearing vector, every bearing measurement in g must be a unit-norm vector. In addition, the bearing vector should also be realizable with the underlying graph $\mathcal{G}$. Thus, the set $\mathcal{X}(\mathcal{G}, \mathrm{g})$ including all the bearing vectors g satisfying these requirements can be defined as the intersection of three sets:

$$\mathcal{X}(\mathcal{G}, \mathrm{g}) = \mathcal{X}_{eq}(\mathcal{G}, \mathrm{g}) \bigcap \mathcal{C}_{norm} \bigcap \mathcal{C}_{realizable}(\mathcal{G}) \tag{21}$$

with

$$\mathcal{X}_{eq}(\mathcal{G}, \mathrm{g}) = \{x \in \mathbb{R}^{2|\mathcal{E}|} : \dot{p} = u(x, \mathrm{g}) = 0\}; \tag{22}$$

$$\mathcal{C}_{norm} = \left\{ g = \begin{bmatrix} g_1 \\ \vdots \\ g_{|\mathcal{E}|} \end{bmatrix} \in \mathbb{R}^{2|\mathcal{E}|} : \|g_k\| = 1, \forall k = 1, \cdots, |\mathcal{E}| \right\}; \tag{23}$$

$$\mathcal{C}_{realizable}(\mathcal{G}) = \{g \in \mathbb{R}^{2|\mathcal{E}|} : \exists p \in \mathbb{R}^{2|\mathcal{V}|}, \text{ such that } g = F_B(p)\}. \tag{24}$$

With more than two terms in $\sum_{j=1}^{n} P_{g_{cj}} \mathrm{g}_{cj}$, it becomes much more difficult to obtain a simple and meaningful solution from the the nonlinear system. The analytical method used to prove Lemma 5 is not practical. The sum $-\sum_{j=1}^{n} P_{g^*_{cj}} \mathrm{g}_{cj}$ equals to zero can not conclude each additive term $P_{g^*_{cj}} \mathrm{g}_{cj}, \forall j = j, \cdots, n$ equals to zero.

From the control system (19), it can be found the control law is linear in the target bearing g but nonlinear in the bearing measurement g. Thus, we alter the problem as following which helps to analyze equilibrium set $\mathcal{X}_{eq}$.

For the agent v_c controlled as (20) with $n \geq 2$, suppose that the target bearing g is *unknown*, nonetheless, the current configuration p is *given* and the current bearing measurement g can be obtained by $F_B(p)$. This time, we aim to determine the target bearing vector g leading the control input $u_c(g, \mathrm{g})$ to be zero. As before, the target set can be expressed by the intersection of three sets:

$$\mathcal{Y}(\mathcal{G}, g) = \mathcal{Y}_{eq}(\mathcal{G}, g) \bigcap \mathcal{C}_{norm} \bigcap \mathcal{C}_{realizable}(\mathcal{G}), \tag{25}$$

where

$$\mathcal{Y}_{eq}(\mathcal{G}, g) = \{\mathrm{y} \in \mathbb{R}^{2|\mathcal{E}|} : \dot{p} = u(g, \mathrm{y}) = 0\}. \tag{26}$$

Before working out $\mathcal{Y}(\mathcal{G}, g)$, we want to explain the relation between $\mathcal{Y}(\mathcal{G}, g)$ and $\mathcal{X}(\mathcal{G}, \mathrm{g})$.

Lemma 6. *Assume that* $g, \mathrm{g} \in \mathcal{C}_{norm} \bigcap \mathcal{C}_{realizable}(\mathcal{G})$. *Then the following statements hold:*

i) $\mathrm{g} \in \mathcal{X}(\mathcal{G}, \mathrm{g})$;

ii) $g \in \mathcal{Y}(\mathcal{G}, g)$.

Proof. Lemma 6 can be verified by the property of projection matrix, $P_x x = 0$. When $g = \mathrm{g}$, the control input (20) $u_c(g, \mathrm{g}) = -\sum_{j=1}^{n} P_{g_{cj}} \mathrm{g}_{cj}$ equals to zero, indicating that $\mathrm{g} \in \mathcal{X}_{eq}(\mathcal{G}, \mathrm{g})$ and $g \in \mathcal{Y}_{eq}(\mathcal{G}, g)$. Furthermore, the bearing vectors g and g are assumed to be in set $\mathcal{C}_{norm} \bigcap \mathcal{C}_{realizable}(\mathcal{G})$. It is sufficient to conclude that $\mathrm{g} \in \mathcal{X}(\mathcal{G}, \mathrm{g})$ and $g \in \mathcal{Y}(\mathcal{G}, g)$. □

These solutions which always exist in the equilibrium set are called the desired solutions since it meets the requirement of the formation control problem (Problem 2). It should be mentioned that actually when $g_{cj} = \pm \mathrm{g}_{cj}$ for every components of the bearing vectors g and g, the control input (20) $u_c(g, \mathrm{g}) = -\sum_{j=1}^{n} P_{g_{cj}} \mathrm{g}_{cj}$ equals to zero due to the property of the projection matrix. However, these combinations may not exist in $\mathcal{C}_{realizable}(\mathcal{G})$ for the sensing graph $\mathcal{G}$ in 1-to-many system.

Lemma 7. *In the 1-to-many system, if* $\mathcal{Y}(\mathcal{G}, g) = \{g\}$ *for any bearing vector* $g \in \mathcal{C}_{norm} \bigcap \mathcal{C}_{realizable}(\mathcal{G})$, *then* $\mathcal{X}(\mathcal{G}, \mathrm{g}) = \{\mathrm{g}\}$ *for any target bearing vector* $\mathrm{g} \in \mathcal{C}_{norm} \bigcap \mathcal{C}_{realizable}(\mathcal{G})$.

Proof. We aim to prove the lemma by contradiction. Suppose for $\mathcal{X}(\mathcal{G}, \mathrm{g})$, there exists another element g', other than the desired element g. That is, assume $\mathcal{X}(\mathcal{G}, \mathrm{g}) = \{\mathrm{g}, \mathrm{g}'\}$, indicating that $\dot{p}_c = u_c(\mathrm{g}', \mathrm{g}) = 0$. Now, consider $\mathcal{Y}(g = \mathrm{g}')$. It includes at least two elements: g', g, since $u_c(\mathrm{g}', \mathrm{g}') = 0$ always holds and $u_c(\mathrm{g}', \mathrm{g}) = 0$ as shown in the last paragraph. The existence of the second element for $\mathcal{Y}(\mathrm{g}')$ contradicts the assumption. □

With the Lemma 6 and Lemma 7, we obtained that the desired solution g always exists in the equilibrium set $\mathcal{X}(\mathcal{G}, \mathrm{g})$ and it would be the only element if $\mathcal{Y}(\mathcal{G}, g) = \{g\}$.

In the following paragraphs, we aim to find out whether there exists other elements for set $\mathcal{Y}(\mathcal{G}, g)$. It is defined as the intersection of three sets (25), thus, the analysis is proceeded with three steps: *i*) find $\mathcal{Y}_{eq}(\mathcal{G}, g)$; *ii*) find $\mathcal{Y}_{eq}(\mathcal{G}, g) \bigcap \mathcal{C}_{norm}$; *iii*) find $\mathcal{Y}_{eq}(\mathcal{G}, g) \bigcap \mathcal{C}_{norm} \bigcap \mathcal{C}_{realizable}(\mathcal{G})$.

We start from looking for the elements in $\mathcal{Y}_{eq}(\mathcal{G}, g)$. Define $\tilde{P}$ as

$$\tilde{P} = \begin{bmatrix} P_{g_{c1}} P_{g_{c2}} \cdots P_{g_{cn}} \end{bmatrix}.$$

Then (19) for agent c can be rewritten as:

$$\dot{p}_c = -\sum_{j=1}^{n} P_{g_{cj}} \mathrm{g}_{cj} = \tilde{P}\mathrm{g}. \tag{27}$$

Any vector in the null-space of $\tilde{P}$ satisfies the equilibrium condition, which means

$$\mathcal{Y}_{eq}(\mathcal{G}, g) = \mathrm{Null}(\tilde{P}).$$

In 2-D space, $\tilde{P}$ is in the dimension of $\mathbb{R}^{2\times 2n}$ and its rank is exactly 2. Thus, the dimension of its null space is $2n-2$.

For every bearing measurement $g_k = [(g_k)_x, (g_k)_y]^T$, we define its orthogonal bearing measurement as $g_k^\perp = [-(g_k)_y, (g_k)_x]^T$ such that $g_k^T g_k^\perp = 0$. Then, we choose the following orthogonal bearing vector to g, $g^\perp = [(g_1^\perp)^T, \cdots, (g_m^\perp)^T]^T$. Define $G \in \mathbb{R}^{2n\times n}$ and $G^\perp \in \mathbb{R}^{2n\times n}$ as the block diagonal matrix of the bearing vector g and its orthogonal vector $g^\perp$,

$$G = \mathrm{diag}(g) = \begin{bmatrix} g_{c1} & 0 & 0 & \cdots & 0 \\ 0 & g_{c2} & 0 & \cdots & 0 \\ 0 & 0 & g_{c3} & \ddots & 0 \\ \vdots & \vdots & \ddots & \ddots & \vdots \\ 0 & 0 & 0 & \cdots & g_{cn} \end{bmatrix}; \tag{28}$$

$$G^\perp = \mathrm{diag}(g^\perp) = \begin{bmatrix} g_{c1}^\perp & 0 & 0 & \cdots & 0 \\ 0 & g_{ic}^\perp & 0 & \cdots & 0 \\ 0 & 0 & g_{c3}^\perp & \ddots & 0 \\ \vdots & \vdots & \ddots & \ddots & \vdots \\ 0 & 0 & 0 & \cdots & g_{cn}^\perp \end{bmatrix}. \tag{29}$$

It is obvious that $\mathrm{Range}(G)$ and $\mathrm{Range}(G^\perp)$ are orthogonal to each other. The direct sum of these two range space $\mathrm{Range}(G) \oplus \mathrm{Range}(G^\perp)$ is exactly the $\mathbb{R}^{2n\times 2n}$ space. The following lemma shows some property of G and $G^\perp$ with respect to $\tilde{P}$.

Lemma 8. *Consider G and $G^\perp$ defined in* (28) *and* (29) *respectively. Then*

i) $\tilde{P}G = \mathbb{0}_{2\times n}$;

ii) $\tilde{P}G^\perp = \begin{bmatrix} g_{c1}^\perp & g_{c2}^\perp & \cdots & g_{cn}^\perp \end{bmatrix}$.

Proof. The proof follows by direct construction. For part *i*) , we have that $P_{g_{ci}} g_{ci} = \mathbb{0}_2$ implies

$$\begin{aligned} \tilde{P}G &= \begin{bmatrix} P_{g_{c1}} g_{c1} & P_{g_{c2}} g_{c2} & \cdots & P_{g_{cn}} g_{cn} \end{bmatrix} \\ &= \begin{bmatrix} \mathbb{0}_2 & \mathbb{0}_2 & \cdots & \mathbb{0}_2. \end{bmatrix} = \mathbb{0}_{2\times n}. \end{aligned}$$

Similarly, for *ii*) we have $P_{g_{ci}} g_{ci}^{\perp} = g_{ci}^{\perp}$ implies

$$\begin{aligned}\tilde{P}G^{\perp} &= \begin{bmatrix} P_{g_{c1}} g_{c1}^{\perp} & P_{g_{c2}} g_{c2}^{\perp} & \cdots & P_{g_{cn}} g_{cn}^{\perp} \end{bmatrix} \\ &= \begin{bmatrix} g_{c1}^{\perp} & g_{c2}^{\perp} & \cdots & g_{cn}^{\perp} \end{bmatrix}.\end{aligned}$$

□

Lemma 8(*i*) indicates that Range(G) ⊂ Null($\tilde{P}$). As discussed previously, the dimension of Null($\tilde{P}$) should be $2n-2$. The columns of G helps to determine n basis vectors of Null($\tilde{P}$) and there are $(n-2)$ basis vectors left to be determined. These basis vectors should be orthogonal to G, which can be expressed by the linear combination of the columns of $G^{\perp}$.

Consider the matrix $\tilde{P}G^{\perp} = \begin{bmatrix} g_{c1}^{\perp}, g_{c2}^{\perp}, \cdots, g_{cn}^{\perp} \end{bmatrix} \in \mathbb{R}^{2\times n}$. Define $N \in \mathbb{R}^{n\times(n-2)}$ which spans the null space of $\tilde{P}G^{\perp}$, i.e., $\tilde{P}G^{\perp}N = \mathbb{0}_{2\times(n-2)}$, from which it can be shown that $G^{\perp}N$ is in the null space of $\tilde{P}$. The dimension of $G^{\perp}N$ is in $\mathbb{R}^{2n\times(n-2)}$, which is exactly the rest of the basis vectors. Thus, we conclude that

$$\text{Null}(\tilde{P}) = \text{Range}(G) \oplus \text{Range}(G^{\perp}N).$$

The equilibrium set $\mathcal{Y}_{eq}(\mathcal{G}, g)$ is included in the null space of $\tilde{P}$ which is well defined by the columns of the matrix G and $G^{\perp}N$. Thus, the target bearing vector g belonging to the equilibrium set $\mathcal{Y}_{eq}(\mathcal{G}, g)$ can explicitly expressed by the linear combination of these column vectors,

$$\mathcal{Y}_{eq}(\mathcal{G}, g) = \{\mathrm{g} : \mathrm{g} = Ga + G^{\perp}Nb, \forall a \in \mathbb{R}^n, b \in \mathbb{R}^{n-2}\}, \tag{30}$$

where $a = [a_1, \cdots, a_n]^T$ and $b = [b_1, \cdots, b_{n-2}]^T$ are vectors of coefficients. We can also express the target bearing $\mathrm{g} = Ga + G^{\perp}Nb$ of each edge individually as

$$\mathrm{g}_{ci} = a_i g_{ci} + \left(\sum_{j=1}^{n-2} b_j N_{ij} \right) g_{ci}^{\perp}. \tag{31}$$

The second procedure is to find its intersection with $\mathcal{C}_{norm}$. From the definition of g_{ci} and $g_{ci}^{\perp}$, these two vectors are perpendicular to each other. The norm can be calculated as

$$\begin{aligned}\|\mathrm{g}_{ci}\| &= \left(a_i g_{ci} + (\sum_{j=1}^{n-2} b_j N_{ij}) g_{ci}^{\perp} \right)^T \left(a_i g_{ci} + (\sum_{j=1}^{n-2} b_j N_{ij}) g_{ci}^{\perp} \right) \\ &= a_i^2 + \left(\sum_{j=1}^{n-2} b_j N_{ij} \right)^2 = 1.\end{aligned} \tag{32}$$

Eventually, the constraint of realizable bearing vectors $\mathcal{C}_{realizable}(\mathcal{G})$ should be taken into consideration. The set $\mathcal{Y}(\mathcal{G}, g)$ is determined by the current bearing

vector g, which is realizable and generated from the current configuration $p = [p_1^T, \cdots, p_n^T, p_c^T]^T$. We denote the position of the fixed agent as $p_0 = [p_1^T, \cdots, p_n^T]^T$. During the full motion, the fixed agents stay at p_0.

For the target bearing vector $\mathrm{g} \in \mathcal{Y}_{eq}(\mathcal{G}, g) \bigcap \mathcal{C}_{norm}$, it is also realizable (i.e., $\mathrm{g} \in \mathcal{C}_{realizable}(\mathcal{G})$) if there exists a target position $\mathrm{p_c}$ for agent c such that the configuration $p = [p_0^T, \mathrm{p}_c^T]^T$ satisfies all the target bearing g.

Lemma 9. *In the 1-to-many system, the bearing vector* $\mathrm{g} \in \mathcal{Y}_{eq}(\mathcal{G}, g) \bigcap \mathcal{C}_{norm}$ *is realizable if and only if* $a = \mathbb{1}_n,\ b = \mathbb{0}_{n-2}$. *Equivalently,*

$$\mathcal{Y}(\mathcal{G}, g) = \mathcal{Y}_{eq}(\mathcal{G}, g) \bigcap \mathcal{C}_{norm} \bigcap \mathcal{C}_{realizable}(\mathcal{G}) = \{g\}.$$

Proof. It can be easily shown that $a = \mathbb{1}_n,\ b = \mathbb{0}_{n-2}$ indicates $\mathrm{g} = Ga + G^{\perp}Nb$ is realizable. The main work is to prove that the realizablitiy of $\mathrm{g} = Ga + G^{\perp}Nb$ requires $a = \mathbb{1}_n,\ b = \mathbb{0}_{n-2}$. We aim to prove by contradiction. Suppose that there exist $a \neq \mathbb{1}_n$, and $b \neq \mathbb{0}_{n-2}$ such that the bearing vector $\mathrm{g} = Ga + G^{\perp}Nb$ is realizable (while the norm constraint is satisfied). The bearing vector g is realizable indicates that there exists a position $\bar{p}_c$ for agent v_c, such that the configuration $\mathrm{p} = [p_0^T, \bar{p}_c^T]$ satisfies all the bearing vector g (i.e.,$\mathrm{p} = F_B^{-1}(g)$).

The displacement measurement (introduced in Section 2.1) between p_c and $\bar{p}_c$ is defined as $z_{\bar{c}c} = p_c - \bar{p}_c$, it can also be rewritten as $z_{\bar{c}c}(i) = z_{\bar{c}i} + z_{ic}, \forall v_i \in \mathcal{V}_0$ where $z_{\bar{c}i} = p_i - \bar{p}_c$ and $z_{ic} = p_c - p_i$. Moreover, we can express $z_{\bar{c}i}$ and z_{ic} as

$$\begin{aligned} z_{\bar{c}c}(i) &= z_{\bar{c}i} + z_{ic} \\ &= d_{\bar{c}i}\mathrm{g}_{ci} - d_{ci}g_{ci} \\ &= (d_{\bar{c}i}a_i - d_{ci})g_{ci} + \left(\sum_{j=1}^{n-2} b_j N_{ij}\right) d_{\bar{c}i} g_{ci}^{\perp}. \end{aligned} \tag{33}$$

It can be observed that $z_{\bar{c}c}(i)$ is expressed by the pair of basis vectors $g_{ci}, g_{ci}^{\perp}$, for all $i = 1, \cdots, n$. Multiplying on the left by $z_{\bar{c}c}(i)^T$ of $\left(\sum_{j=1}^{n-2} b_j N_{ij}\right) g_{ci}^{\perp}$ gives

$$z_{\bar{c}c}(i)^T \left(\sum_{j=1}^{n-2} b_j N_{ij}\right) g_{ci}^{\perp} = \left(\sum_{j=1}^{n-2} b_j N_{ij}\right)^2 d_{\bar{c}i} \geq 0. \tag{34}$$

The last inequality holds since the distance $d_{\bar{c}i}$ is in $\mathbb{R}_{>}$. This inequality holds for all $i = 1, \cdots, n$.

On the other hand, it should be mentioned that the following equation always holds since $(\mathbb{1}_n^T \otimes I_2)G^{\perp} = \tilde{P}G^{\perp} = [g_{c1}^{\perp}, \cdots, g_{cn}^{\perp}]$,

$$(\mathbb{1}_n^T \otimes I_2)G^{\perp}Nb = \tilde{P}G^{\perp}Nb = \mathbb{0}_2 \Leftrightarrow \sum_{i=1}^{n} \left(\sum_{j=1}^{n-2} b_j N_{ij}\right) g_{ci}^{\perp} \ = \mathbb{0}_2 \tag{35}$$

Any vector multiplied by zero is zero, which leads to

$$z_{\bar{c}c}^T \sum_{i=1}^{n} \left(\sum_{j=1}^{n-2} b_j N_{ij} \right) g_{ci}^{\perp} = 0 \Leftrightarrow \sum_{i=1}^{n} \left([z_{\bar{c}c}(i)^T \left(\sum_{j=1}^{n-2} b_j N_{ij} \right) g_{ci}^{\perp} \right) = 0. \tag{36}$$

With each additive term $z_{\bar{c}c}(i)^T \left(\sum_{j=1}^{n-2} b_j N_{ij} \right) g_{ci}^{\perp}$ greater or equal to zero (34), the sum equals to zero (35) implies that each additive term should be exactly zero, which requires that $z_{\bar{c}c} = \mathbb{0}_2$ because the vectors $g_{ci}^{\perp}, \forall i = 1, \cdots, n$ are not collinear with each other.

The displacement measurement $z_{\bar{c}c} = \mathbb{0}_2$ indicates that

$$(d_{\bar{c}i} a_i - d_{ci}) g_{ci} + (\sum_{j=1}^{n-2} b_j N_{ij}) d_{\bar{c}i} g_{ci}^{\perp} = \mathbb{0}_2, \forall i = 1, \cdots, n.$$

The basis vector g_{ci} and $g_{ci}^{\perp}$ are perpendicular to each other, thus, the coefficients $d_{\bar{c}i} a_i - d_{ci}$ and $\sum_{j=1}^{n-2} (b_j N_{ij}) d_{\bar{c}i}$ equal to zero individually.

With the distance d_{ci} and $d_{\bar{c}i}$ taken in $\mathbb{R}_>$, we can conclude that $a_i > 0$ and $\sum_{j=1}^{n-2} b_j N_{ij} = 0$ for all $i = 1, \cdots, n$. Moreover, all the columns of the matrix N are linear independent, the matrix $Nb = \mathbb{0}_n$ requires $b = \mathbb{0}_{n-2}$. Finally, the norm constraint gives that $a = \mathbb{1}_n$. □

As a conclusion, Lemma 9 shows that $\mathcal{Y}(\mathcal{G}, g) = \{g\}$. Then, we can obtain $\mathcal{X}(\mathcal{G}, \mathrm{g}) = \{\mathrm{g}\}$ from Lemma 7. For the 1-to-many system with $n > 2$ outgoing edges for agent c (19), the system reaches equilibrium when the current bearing vector g coincides with the target bearing vector g. The position p_c^* can be uniquely defined by the equilibrium condition $g^* = \mathrm{g}$ and the initial condition of the fixed agents, which is $p_c^* = \left(\sum_{j \in \mathcal{N}_i} P_{\mathrm{g}_{ij}} \right)^{-1} \left(\sum_{j \in \mathcal{N}_i} P_{\mathrm{g}_{ij}} p_j(t_0) \right)$. Combined with the positions of the fixed agents, the equilibrium configuration can be expressed as: $p^* = F_B^{-1}(\mathrm{g}) = \left[(p_0(t_0))^T, (p_c^*)^T \right]$.

The last step is to determine the stability of equilibrium.

Lemma 10. *The system equilibrium $p^* = \left[(p_0(t_0))^T, (p_c^*)^T \right]$ is asymptotically stable. In other words, in the 1-to-many system with more than two leaders, the agent v_c asymptotically converges to the equilibrium $p_c^* = \left(\sum_{j \in \mathcal{N}_i} P_{\mathrm{g}_{ij}} \right)^{-1} \left(\sum_{j \in \mathcal{N}_i} P_{\mathrm{g}_{ij}} p_j(t_0) \right)$.*

Proof. Consider the Lyapunov function: $V(t) = \frac{1}{2}\|p_c(t) - p_c^*\|^2$. Then

$$\begin{aligned}
\dot{V} &= (p_c - p_c^*)^T \dot{p}_c \\
&= -(p_c - p_c^*)^T \sum_{i=1}^{n} P_{g_{ci}} g_{ci}^* \\
&= -(p_c - p_c^*)^T \sum_{i=1}^{n} \frac{P_{g_{ci}}}{d_{ci}} (p_i - p_c^*) \\
&= -(p_c - p_c^*)^T \sum_{i=1}^{n} \frac{P_{g_{ci}}}{d_{ci}} (p_i - p_c + p_c - p_c^*) \\
&= -(p_c - p_c^*)^T \left(\sum_{i=1}^{n} \frac{P_{g_{ci}}}{d_{ci}} (p_c - p_c^*) \right) \\
&= -(p_c - p_c^*)^T \underbrace{\left(\sum_{i=1}^{n} \frac{P_{g_{ci}}}{d_{ci}} \right)}_{M} (p_c - p_c^*) \leq 0.
\end{aligned} \tag{37}$$

The projection matrix $P_{g_{ci}}$ is positive semi-definite. Thus, the matrix $M = \sum_{i=1}^{n} \frac{P_{g_{ci}}}{d_{ci}} \geq 0$, indicating $\dot{V}(t) \leq 0$ during the motion.

Moreover, $\dot{V} = 0$ if and only if $(p_c(t) - p_c^*) \in \text{Null}(M(t))$, where the null space of M can be considered in two cases:

i) If $p_c(t)$ is collinear with all the fixed agents, i.e., the bearing measurements $g_{c1}, g_{c2}, \cdots, g_{cn}$ are parallel and the projection matrix $P_{g_{c1}} = P_{g_{c2}} = \cdots = P_{g_{cn}}$, then the matrix M can be simplified as $M = P_{g_{c1}} \left(\sum_{i=1}^{n} \frac{1}{d_{ci}} \right)$ and the space $\text{Null}(M) = \{g_{c1}\}$ (7). From Assumption 3, any two target bearing $g_{ci}, g_{cj}, v_{i,j} \in \mathcal{V}_0$ are not parallel, implying that $p_c^* = p_c$ is not collinear with any two other fixed agents. Thus, $(p_c(t) - p_c^*)$ is not parallel with the bearing measurement g_{c1} and $(p_c(t) - p_c^*)$ is not in the space $\text{Null}(M(t))$.

ii) If $p_c(t)$ is not collinear with all the fixed agents, i.e., there exists $v_{i,j} \in \mathcal{V}_0$ such that $p_c(t), p_i, p_j$ are not collinear and the bearing measurements g_{ci} and g_{cj} are not parallel. The sum of the projection matrices $P_{g_{ci}} + P_{g_{cj}}$ is invertible and positive definite (see the proof of Lemma 3). With all the other additive terms to be positive semi-definite, the matrix M is positive definite. In this case, $\dot{V} = 0$ if and only if $p_c(t) - p_c^* = 0$.

As a result, $\dot{V}(t) \leq 0$ and the equality holds when $p_c(t)$ reaches the equilibrium p_c^*. Consequently, the equilibrium $p^* = \left[(p_0(t_0))^T, (p_c^*)^T \right]$ is GAS. □

In conclusion, for the 1-to-many system with $n > 2$, the agent v_c asymptotically converges to the target position which satisfies the target formation along with the positions of the leaders.

Next, we will illustrate the null space analysis of $\tilde{P}$ with an example.

Example 7. *Consider the current configuration for the fixed agents and agent c shown in Figure 20. The current bearing measurement can be obtained as $g_{c1} = [-1, 0]^T, g_{c2} = [-\frac{\sqrt{2}}{2}, -\frac{\sqrt{2}}{2}]^T, g_{c3} = [\frac{\sqrt{2}}{2}, -\frac{\sqrt{2}}{2}]^T, g_{c4} = [0, 1]^T$. Then, the orthogonal vector to each bearing measurement can be expressed as $g_{c1}^\perp = [0, -1]^T, g_{c2}^\perp = [\frac{\sqrt{2}}{2}, -\frac{\sqrt{2}}{2}]^T, g_{c3}^\perp = [-\frac{\sqrt{2}}{2}, -\frac{\sqrt{2}}{2}]^T, g_{c4}^\perp = [-1, 0]^T$.*

The matrix N can be acquired by the null space of matrix

$$\begin{bmatrix} g_{c1}^\perp & g_{c2}^\perp & g_{c3}^\perp & g_{c4}^\perp \end{bmatrix} = \begin{bmatrix} 0 & \frac{\sqrt{2}}{2} & -\frac{\sqrt{2}}{2} & -1 \\ -1 & -\frac{\sqrt{2}}{2} & -\frac{\sqrt{2}}{2} & 0 \end{bmatrix}.$$

The null space analysis gives that

$$N = \begin{bmatrix} -\sqrt{2} & -1 \\ 1 & \sqrt{2} \\ 1 & 0 \\ 0 & 1 \end{bmatrix}.$$

Then, the basis vector of the subspace $\mathrm{Null}(\tilde{P})$ *can be determined by the columns of matrices G and $G^\perp N$*

$$\mathrm{Null}(\tilde{P}) = \mathrm{span}\left\{ \begin{bmatrix} g_{c1} \\ 0 \\ 0 \\ 0 \end{bmatrix} \begin{bmatrix} 0 \\ g_{c2} \\ 0 \\ 0 \end{bmatrix} \begin{bmatrix} 0 \\ 0 \\ g_{c3} \\ 0 \end{bmatrix} \begin{bmatrix} 0 \\ 0 \\ 0 \\ g_{c4} \end{bmatrix} \begin{bmatrix} -\sqrt{2}g_{c1}^\perp \\ g_{c2}^\perp \\ g_{c3}^\perp \\ 0 \end{bmatrix} \begin{bmatrix} -g_{c1}^\perp \\ \sqrt{2}g_{c2}^\perp \\ 0 \\ g_{c4}^\perp \end{bmatrix} \right\}. \tag{38}$$

The vector g *satisfying $\dot{p}_c = u_c(g, \mathrm{g}) = 0$ is in the subspace* $\mathrm{Null}(\tilde{P})$*, which can be expressed by the linear combination of the basis vectors as following with the coefficients a_i and b_j,*

$$\begin{aligned} \mathrm{g}_{c1} &= a_1 g_{c1} + (-\sqrt{2}b_1 - b_2) g_{c1}^\perp \\ \mathrm{g}_{c2} &= a_2 g_{c2} + (b_1 + \sqrt{2}b_2) g_{c2}^\perp \\ \mathrm{g}_{c3} &= a_3 g_{c3} + b_1 g_{c3}^\perp \\ \mathrm{g}_{c4} &= a_4 g_{c4} + b_2 g_{c4}^\perp \end{aligned}. \tag{39}$$

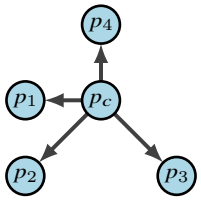

Figure 20: The sensing graph and current configuration for the illustrating example.

Or in matrix form,

$$\mathrm{g} = \begin{bmatrix} G & G^{\perp}N \end{bmatrix} \begin{bmatrix} a \\ b \end{bmatrix} = \begin{bmatrix} g_{c1} & 0 & 0 & 0 \\ 0 & g_{c2} & 0 & 0 \\ 0 & 0 & g_{c3} & 0 \\ 0 & 0 & 0 & g_{c4} \end{bmatrix} \begin{bmatrix} a_1 \\ a_2 \\ a_3 \\ a_4 \end{bmatrix} + \begin{bmatrix} -\sqrt{2}g_{c1}^{\perp} & -g_{c1}^{\perp} \\ g_{c2}^{\perp} & \sqrt{2}g_{c2}^{\perp} \\ g_{c3}^{\perp} & 0 \\ 0 & g_{c4}^{\perp} \end{bmatrix} \begin{bmatrix} b_1 \\ b_2 \end{bmatrix}. \quad (40)$$

Constraints on the coefficients should be made to ensure the norm of each bearing measurement to be 1*,*

$$\begin{aligned} a_1 &= \pm\sqrt{1-(-\sqrt{2}b_1 - b_2)^2} \\ a_2 &= \pm\sqrt{1-(b_1 + \sqrt{2}b_2)^2} \\ a_3 &= \pm\sqrt{1-b_1^2} \\ a_4 &= \pm\sqrt{1-b_2^2} \end{aligned}$$

Note that b_1, b_2 *can only vary in the range assuring that* a_1, a_2, a_3, a_4 *are real.*

A simulation example is performed to verify the analysis of the 1-to-many system with more than two leaders.

Example 8. *We choose to simulate the 1-to-many system with* 5 *outgoing edges for agent* v_c*. In this simulation, the target bearing is chosen as Figure 21a. The positions of the leaders are chosen to satisfy the assumption 4, which is* $p_i = \left[\cos\left(\frac{2i}{5}\pi\right), \sin\left(\frac{2i}{5}\pi\right)\right]^T$*, for* $i = 1, \cdots, 5$*. A target position of agent* v_c *can be localized by target bearing vector* g *and the position of fixed agents* p_0 *as* $\mathrm{p}_c = [0, 0]^T$*. The random initial position for agent* v_c *is taken as* $p_c(t_0) = [0.8147, 0.9058]^T$*. Figure 21b depicts the trajectory and the final position of the agent* c*, which demonstrates that the agent* c *converges to the target position. Figure 21c then verifies that the bearing error converges to zero asymptotically.*

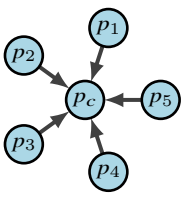

(a) The target bearing formation.

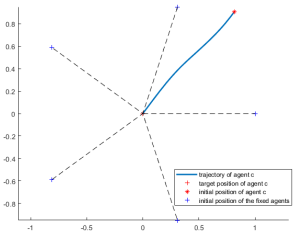

(b) System trajectories.

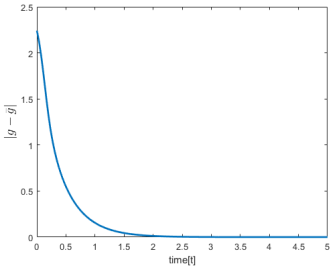

(c) Bearing error along the system trajectories.

Figure 21: Simulation result of bearing-only formation control system with target bearing formation as Figure 21a.

3.4 BOFC with LFF Graphs

In last section, we presented the idea to analyze the performance of each agent individually. After acknowledging the behavior of 1-to-many system controller by BOFC, we are well prepared to work on the system with more general sensing graphs. In this section, we will propose some conditions on the directed graphs which solves Problem 3 and then prove the MAS with such sensing graphs can be brought to the target bearing formation by BOFC.

Ordered LFF Graphs.

Recall that in the Section 2.3, the leader first-follower graph generated from Henneberg construction has been introduced. We use the abbreviation HCLFF graph in the following text. The most essential property of HCLFF graphs is orderliness, which directly leads to the occurrence of triangular structure in the system controlled with BOFC. Applying the stability theorem of cascade system, the stability analysis of equilibrium can be developed step by step.

A reasonable method to extend the universality is adding edge to the formation. We prefer to keep the leader and first follower since it helps to uniquely define the scale and position of the framework.

The HCLFF graph can be expanded by adding some additional edges to the graph. The orderliness property is kept if and only if all the additional edges are forward edges. If the orderliness still exists, the stability of equilibrium analysis can be performed with the same method as introduced in Section 2.3.

Definition 12. *An ordered LFF graph $\mathcal{G}$ is a directed graph such that*

i) There exists a leader and a first-follower.

ii) All the edges are forward edges.

iii) Every vertex other than the leader and the first follower has at least two outgoing edges.

In Section 3.1, Figure 15a shows an example of target bearing formation whose underlying graph is ordered LFF graph. The ordered LFF graph consists of a HCLFF subgraph and some forward edges. The extended ordered LFF graph is still generically bearing rigid. For the target bearing formation $(\mathcal{G}, \mathrm{g})$ whose underlying graph is ordered LFF graph, the target configuration p satisfying target bearing vector g can be uniquely determined according to the HCLFF subgraph and the initial condition of $p_1(t_0), d_{21}(t_0)$ (Lemma 2). On the other hand, since all the edges are forward edges, the orderliness in the structure is remained. Note that for agent v_3, there are only two agents with smaller label, which are the leader v_1 and first follower v_2. Owning at least two forward edges indicates that agent v_3 has exactly two outgoing edges towards agents v_1 and v_2.

Theorem 5. *The ordered LFF graphs solve Problem 3. In other words, the bearing-only formation control* (13) *asymptotically drives the MAS with ordered LFF sensing (Def. 12) to the target formation.*

Before the proof of Theorem 5, we primarily show that the cascade structure still occurs since the property of orderliness is maintained in the ordered LFF graph.

The whole multi-agent bearing-only formation control system with the ordered LFF graph (as Figure 22) can be written as

$$\begin{bmatrix} \dot{p}_1 \\ \dot{p}_2 \\ \dot{p}_3 \\ \vdots \\ \dot{p}_n \end{bmatrix} = \begin{bmatrix} u_1(p_1) \\ u_2(p_1, p_2) \\ u_3(p_1, p_2, p_3) \\ \vdots \\ u_n(p_1, p_2, p_3, \cdots, p_{n-1}, p_n) \end{bmatrix}, \tag{41}$$

where $u_i = -\sum_{j\in\mathcal{N}_i} P_{g_{ij}} g_{ij}$ is the bearing-only formation control law. From the above equations, it can be observed that the triangular structure appears.

Proof. The equilibrium and stability analysis can be performed step by step with the order from the leader agent v_1 to the last agent v_n. For agent v_1, there is no outgoing edge. The corresponding dynamics are $\dot{p}_1 = u_1 = 0$, giving that the leader is fixed at the initial position which is also the equilibrium for the leader $p_1^* = p_1(t_0)$.

For the first follower (agent v_2), its corresponding dynamic equation is $\dot{p}_2 = u_2(p_1, p_2)$. Since the equilibrium position for agent v_1 has already been determined as p_1^*, the equilibrium analysis for the first follower v_2 focuses on the following system,

$$\dot{p}_2 = u_2(p_1^*, p_2) = -P_{g_{21}} g_{21}. \tag{42}$$

The system is the 1-to-many system with one outgoing edge. The system convergence is concluded in Lemma 4. Two equilibrium exist for agent v_2, which are $p_{2a}^* = p_1^* - d_{21} g_{21} = p_2$ and $p_{2b}^* = p_1^* + d_{21} g_{21}$. The agent v_2 will asymptotically converges to the desired equilibrium p_{2a}^* if the initial condition $p_2(t_0)$ does not coincide with p_{2b}^*.

For the agents other than the leader and the first follower, all of them have at least two forward edges, which can be dealt with the similar process. The analysis of agent v_3 is given in detail as an example for all these agents other than the LFF.

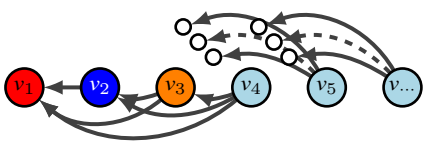

Figure 22: Illustrating graph to show the orderliness in an ordered LFF graph.

Agent v_3 dynamics can be written as $\dot{p}_3 = u_3(p_1, p_2, p_3)$. The equilibrium for agent v_1 and v_2 has been solved and divided into two possibilities as p_1^*, p_{2a}^* and p_1^*, p_{2b}^*. The equilibrium analysis for agent v_3 can be performed on the following two systems individually:

$$\text{system 3a: } \dot{p}_{3a} = u_3(p_1^*, p_{2a}^*, p_{3a});$$
$$\text{system 3b: } \dot{p}_{3b} = u_3(p_1^*, p_{2b}^*, p_{3b}).$$

The system 3a is the 1-to-many system with two outgoing edges. In this system, agents v_1 and v_2 are fixed at p_1^* and p_{2a}^*. Its convergence has been concluded in Lemma 5. There exists a unique GAS equilibrium $p_{3a}^* = (P_{\mathrm{g}_{31}} + P_{\mathrm{g}_{32}})^{-1}(P_{\mathrm{g}_{31}} p_1^* + P_{\mathrm{g}_{32}} p_{2a}^*)$.

For system 3b, it is also the 1-to-many system with two outgoing edges. However, Assumption 4 is not satisfied since the target bearing g_{31} and g_{32} is not realizable with v_1 and v_2 fixed at p_1^* and p_{2b}^*. An illustration example is given in Figure 23. The Assumption 4 is not satisfied since there does not exist any position p_3 such that the configuration $p = [(p_1^*)^T, (p_{2b}^*)^T, (\mathrm{p}_3)^T]^T$ satisfies the target bearing $\mathrm{g}_{31}, \mathrm{g}_{32}$. Thus, the result of 1-to-many system with two outgoing edges can not be applied directly.

Consider another 1-to-many system denoted as system 3c. In system 3c, the fixed agents (leaders) v_1 and v_2 locate at p_1^* and p_{2b}^* and the follower agent v_3 is controlled by BOFC (13). The target bearing vector is chosen as $\mathrm{g} = [-\mathrm{g}_{31}^T, -\mathrm{g}_{31}^T]^T$ such that the Assumption 4 is satisfied. Then, the dynamic of agent v_3 in system 3c is

$$\text{system 3c: } \dot{p}_{3c} = u_3(p_1^*, p_{2b}^*, p_{3c}) = P_{g_{31}} g_{31} + P_{g_{32}} g_{32}.$$

The Lemma 5 can be applied to conclude that the system 3c has a unique GAS equilibria at $p_{3c}^* = (P_{\mathrm{g}_{31}} + P_{\mathrm{g}_{32}})^{-1}(P_{\mathrm{g}_{31}} p_1^* + P_{\mathrm{g}_{32}} p_{2b}^*)$. On the other hand, the dynamics of agent v_3 in system 3b can be expressed as

$$\dot{p}_{3b} = u_3(p_1^*, p_{2b}^*, p_{3b}) = -P_{g_{31}} g_{31} - P_{g_{32}} g_{32}.$$

Comparing with system 3c, the system 3b and system 3c are actually two autonomous systems with completely opposite dynamic (i.e., $\dot{p}_{3b} = u(p_{3b})$ and $\dot{p}_{3c} = -u(p_{3c})$). Therefore, the system 3b and system 3c share the same equilibrium, which means there exists a unique equilibria for system 3b at

$$p_{3b}^* = p_{3c}^* = (P_{\mathrm{g}_{31}} + P_{\mathrm{g}_{32}})^{-1}(P_{\mathrm{g}_{31}} p_1^* + P_{\mathrm{g}_{32}} p_{2b}^*)$$

.

Furthermore, it can be verified that if x^* is a GAS equilibrium for system $\dot{x} = f(x)$, then x^* is an unstable equilibrium for system $\dot{x} = -f(x)$. For this reason, the equilibrium p_{3b}^* is unstable for the system 3b.

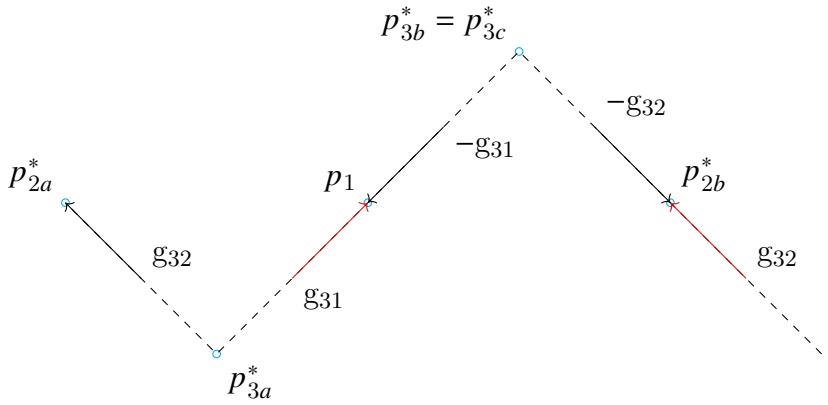

Figure 23: Illustration graph for the equilibrium of system 3a, 3b, 3c.

For the other agents, the analysis is similar to agent v_3 and performed with induction. Consider the agent v_i, $i \in \{3, \dots, n\}$. Its equilibrium analysis can be separated to

$$\text{system } i\text{a: } \dot{p}_{ia} = u_i(p^*_1, p^*_{2a}, \cdots, p^*_{(i-1)a}, p_{ia})$$
$$\text{system } i\text{b: } \dot{p}_{ib} = u_i(p^*_1, p^*_{2b}, \cdots, p^*_{(i-1)b}, p_{ib})$$

The system (ia) is a 1-to-many system with at least two outgoing edges. From Lemma 5 and Lemma 10, there exists only one asymptotically stable equilibrium $p^*_{ia} = \left(\sum_{j\in\mathcal{N}_i} P_{g_{ij}}\right)^{-1} \left(\sum_{j\in\mathcal{N}_i} P_{g_{ij}} p^*_{ja}\right)$ to the system (ia).

The system (ib) is also an 1-to-many system with at least two outgoing edges. The obstacle that the Assumption 4 is not fulfilled still occurs as with system 3b. It can be handled with the same method. The equilibrium of system (ib) is $p^*_{ib} = \left(\sum_{j\in\mathcal{N}_i} P_{g_{ij}}\right)^{-1} \left(\sum_{j\in\mathcal{N}_i} P_{g_{ij}} p^*_{ja}\right)$, which is an unstable equilibrium. After the equilibrium analysis of all agents are carried out, the system equilibrium can be parted into two group $p^*_a = [(p^*_1)^T, (p^*_{2a})^T, \cdots, (p^*_{na})^T]^T$ and $p^*_b = [(p^*_1)^T, (p^*_{2b})^T, \cdots, (p^*_{nb})^T]^T$.

As illustrated in Figure 24, the configuration p^*_a satisfies all the target bearing g and coincides with the target configuration p defined by the $p_1(t_0)$ and $d_{21}(t_0)$.

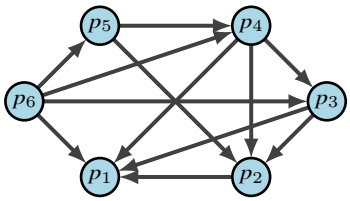

(a) The target formation.

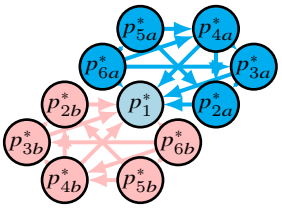

(b) The equilibrium p^*_a and p^*_b corresponding to the target formation 24a.

Figure 24: Illustrating graph for the two groups of equilibrium.

The configuration p_b^* satisfies the negative target bearing $-\mathrm{g}$ and it is symmetric to the target configuration with respect to $p_1(t_0)$. The last step is to prove the stability of the equilibrium. Recall the bearing-only formation control system with the sensing graph described by ordered LFF graph stated in equation (41), the stability theorem of cascade system (Theorem 6) can be applied again and again. Firstly, for the subsystem

$$\dot{p}_1 = 0,$$

The equilibrium $p_1^* = p_1(t_0)$ is stable.

For the subsystem $\dot{p}_2 = u_2(p_1^*, p_2)$, we obtained that p_{2a}^* is an almost GAS equilibria. With the stability theorem of cascade system (Theorem 6), it can be inferred that for the subsystem

$$\begin{bmatrix} \dot{p}_1 \\ \dot{p}_2 \end{bmatrix} = \begin{bmatrix} u_1(p_1) \\ u_2(p_1, p_2) \end{bmatrix},$$

the equilibrium (p_1^*, p_{2a}^*) is almost GAS.

Next, we find that p_{3a}^* is the GAS equilibrium for system $\dot{p}_3 = u_3(p_1^*, p_{2a}^*, p_3)$. It indicates that for the subsystem

$$\begin{bmatrix} \dot{p}_1 \\ \dot{p}_2 \\ \dot{p}_3 \end{bmatrix} = \begin{bmatrix} u_1(p_1) \\ u_2(p_1, p_2) \\ u_3(p_1, p_2, p_3) \end{bmatrix},$$

the equilibrium $(p_1^*, p_{2a}^*, p_{3a}^*)$ is almost GAS.

The procedure can be repeated for the remaining subsystems $\dot{p}_i = u_i(p_1, \ldots, p_i)$ for $i \in \{4, \ldots, n\}$. Consistent with all the agents, we have shown that p_{ia}^* is the GAS equilibrium for subsystem (ia). Eventually, it can be concluded that the equilibrium p_a^* is almost GAS for the BOFC system (41) with ordered LFF sensing graph.

The stability of equilibrium p_b^* can be proved in the same way. The result is that the equilibrium p_b^* is not stable mainly because all the equilibrium p_{ib}^* is unstable. Consequently, the BOFC system (41) with ordered LFF graph converges to the target configuration p which satisfies the target bearing formation $(\mathcal{G}, \mathrm{g})$ in an almost GAS manner. The ordered LFF graph solves the Problem 3. □

Along with the proof, we will present some numerical simulation for the BOFC system with the ordered LFF graphs.

Example 9. *For the multi-agent system of the numerical simulation, the target formation is assigned as Figure 25a. Observe that the directed sensing condition is expressed by an ordered LFF graph. The initial configuration of the system is chosen*

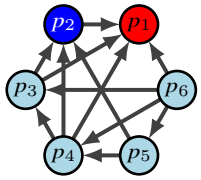

(a) The target bearing formation.

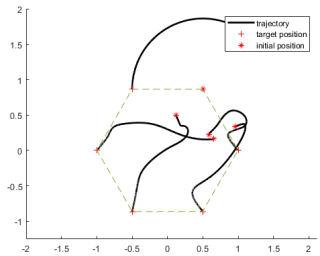

(b) System trajectories.

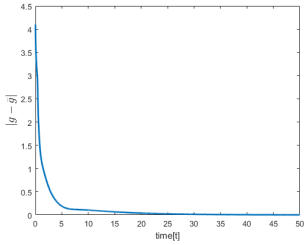

(c) Bearing error along the system trajectories.

Figure 25: Simulation result of bearing-only formation control system with target bearing formation as Figure 25a.

randomly. For this particular example,

$$p(t_0) = [(0.5000, 0.8660), (0.8763, 1.7925), (0.6551, 0.1626), (0.1190, 0.4984), (0.9597, 0.3404), (0.5853, 0.2238)]^T.$$

The agents are controlled with the distributed control scheme, bearing-only formation control (12)*.*

As shown in Figure 25b, the MAS converges to the target bearing formation. Moreover, the Figure 25c indicates that the bearing error between the target bearing and current bearing converges to zero asymptotically.

Disordered LFF Graph.

In Def. 12, the condition of the directed graph for Problem 3 is expanded by adding forward edges. We still regard this extended class of directed graph as not general enough. From Section 3.1, the second trail provides the feasibility of occurrence of the backward edges.

Definition 13. *A disordered LFF graph $\mathcal{G}$ is a directed graph such that:*

i) There exists a leader and a first follower.

ii) For each vertex other than the leader and the first follower, there exists at least two forward outgoing edges.

The disordered LFF graph $\mathcal{G}$ always contains an HCLFF subgraph, implying that $\mathcal{G}$ is generically bearing rigid. For the infinitesimally bearing rigid target bearing formation $(\mathcal{G}, \mathrm{g})$ whose underlying graph $\mathcal{G}$ is disordered LFF graph, the configuration p satisfying target bearing vector g can be uniquely determined according to the HCLFF subgraph and the initial condition of p_1, d_{21}.

We now explore whether the disordered LFF graph is a solution to Problem 3. With the bearing-only formation control law (13) applied on each agent distributively, the control system can be expressed as

$$\dot{p} = u(g, \mathrm{g}) = -\tilde{H}_{out}^T \operatorname{diag}(P_g)\mathrm{g}, \tag{43}$$

where $\tilde{H}_{out} = H_{out} \otimes I_{\mathsf{d}}$.

Compared with Def 12, the appearance of backward edges breaks the triangular structure in the control system. The equilibrium analysis for the system (43) can not be performed step by step.

In system (43), the control input is a function of target measurement and the current measurement: $\dot{p} = u(g, \mathrm{g})$. We aim to look for the equilibrium set $\mathcal{X}(\mathcal{G}, \mathrm{g})$ defined in the same way as (21). However, due to the nonlinearity and asymmetry of the system, it is tedious to work out $\mathcal{X}(\mathcal{G}, \mathrm{g})$. Again, we bring in $\mathcal{Y}(\mathcal{G}, g)$ to deal with the nonlinearity. Similarly as in Section 3.3, the first step is to reveal the relation between sets $\mathcal{X}(\mathcal{G}, \mathrm{g})$ and $\mathcal{Y}(\mathcal{G}, g)$ with the sensing graph $\mathcal{G}$ satisfying Def 13. Then, we will proceed on the set $\mathcal{Y}(\mathcal{G}, g)$.

It can be discovered that the control law $u(g, \mathrm{g}) = \tilde{H}_{out}^T \operatorname{diag}(P_g)\mathrm{g}$ is a symmetric function, i.e., it satisfies $u(g, \mathrm{g}) = u(-g, \mathrm{g})$. Moreover, the control law is linear in the g, leading that $u(g, \mathrm{g}) = -u(g, -\mathrm{g})$. This property gives that if vector x is in $\mathcal{X}_{eq}(\mathcal{G}, \mathrm{g})$ or $\mathcal{Y}_{eq}(\mathcal{G}, g)$ then $-x$ is in $\mathcal{X}_{eq}(\mathcal{G}, \mathrm{g})$ or $\mathcal{Y}_{eq}(\mathcal{G}, g)$.

On the other hand, if the vector x is in $\mathcal{C}_{norm} \bigcap \mathcal{C}_{realizable}(\mathcal{G})$, then $-x$ is also in $\mathcal{C}_{norm} \bigcap \mathcal{C}_{realizable}$. Then, we can conclude that if x is in $\mathcal{X}(\mathcal{G}, \mathrm{g})$ or $\mathcal{Y}(\mathcal{G}, \mathrm{g})$ then $-x$ is in $\mathcal{X}(\mathcal{G}, \mathrm{g})$ or $\mathcal{Y}(\mathcal{G}, \mathrm{g})$, which means the elements of $\mathcal{X}(\mathcal{G}, \mathrm{g})$ and $\mathcal{Y}(\mathcal{G}, g)$ appears in pairs.

Lemma 11. *Assume that $g, \mathrm{g} \in \mathcal{C}_{norm} \bigcap \mathcal{C}_{realizable}(\mathcal{G})$. Then the following statements hold for any disordered LFF graph $\mathcal{G}$:*

i) $\{\mathrm{g}, -\mathrm{g}\} \subseteq \mathcal{X}(\mathcal{G}, \mathrm{g})$;

ii) $\{g, -g\} \subseteq \mathcal{Y}(\mathcal{G}, g)$.

Proof. From the property of projection matrix (7), it can be inferred that $P_{g_{ij}}\mathrm{g}_{ij} = 0$ when $g_{ij} = \pm\mathrm{g}_{ij}$, or equivalently, $\mathrm{g}_{ij} = \pm g_{ij}$. Thus, it can be determined that $\{\mathrm{g}, -\mathrm{g}\} \subseteq \mathcal{X}_{eq}(\mathcal{G}, \mathrm{g})$ and $\{g, -g\} \subseteq \mathcal{Y}_{eq}(\mathcal{G}, g)$.

On the other hand, if the vector g satisfies the norm constraint, meaning that every component of g has norm 1, then the negative vector $-g$ also satisfies the norm constraint. Moreover, if the vector g is realizable in $\mathbb{R}^{\mathsf{d}}$ with the disordered LFF graph $\mathcal{G}$, indicating there exists configuration p such that $F_B(p) = g$. It can be verified that the vector $-g$ is also realizable with the configuration $-p$ (i.e., $F_B(-p) = -g$).

As a result, the bearing vectors g and g are assumed to be in the set $\mathcal{C}_{norm} \bigcap \mathcal{C}_{realizable}(\mathcal{G})$, leading to the fact $-g, -\mathrm{g} \in \mathcal{C}_{norm} \bigcap \mathcal{C}_{realizable}(\mathcal{G})$. It can be concluded that $\{\mathrm{g}, -\mathrm{g}\} \subseteq \mathcal{X}(\mathcal{G}, \mathrm{g})$ and $\{g, -g\} \subseteq \mathcal{Y}(\mathcal{G}, g)$. □

Lemma 12. *For any* $g, \mathrm{g} \in \mathcal{C}_{norm} \bigcap \mathcal{C}_{realizable}$ *and disordered LFF graph* $\mathcal{G}$*, if* $\mathcal{Y}(\mathcal{G}, g) = \{\pm g\}$*, then* $\mathcal{X}(\mathcal{G}, \mathrm{g}) = \{\mathrm{g}\}$*.*

Proof. The Lemma 12 is alike with Lemma 7, the proof can be accomplished by contradiction. Suppose for set $\mathcal{X}(\mathcal{G}, \mathrm{g})$, there exists another pair of elements $\pm x$ (i.e., $\{\pm\mathrm{g}, \pm x\} \subseteq \mathcal{X}(\mathcal{G}, \mathrm{g})$), indicating that $\dot{p} = u(\pm x, \mathrm{g}) = 0$ and $\pm x \in \mathcal{C}_{norm} \bigcap \mathcal{C}_{realizable}(\mathcal{G})$. Then, consider the set $\mathcal{Y}(\mathcal{G}, x)$. Since *i)* $u(x, \mathrm{g}) = 0$; *ii)* $\mathrm{g} \in \mathcal{C}_{norm} \bigcap \mathcal{C}_{realizable}(\mathcal{G})$; *iii*) the elements appear in couple, we have $\pm\mathrm{g}$ in the set $\mathcal{Y}(\mathcal{G}, x)$. Along with $\{\pm x\}$, it can be obtained that $\{\pm\mathrm{g}, \pm x\} \subseteq \mathcal{Y}(\mathcal{G}, x)$, which contradicts the assumption. □

In the following paragraph, the target is to find out the elements in the set $\mathcal{Y}(\mathcal{G}, g)$, which is defined in the intersection of three sets: $\mathcal{Y}_{eq}(\mathcal{G}, g)$, $\mathcal{C}_{norm}$ and $\mathcal{C}_{realizable}(\mathcal{G})$. For any realizable bearing vector g, there exists a configuration $\mathrm{p} \in \mathbb{R}^{2n}$ and a distance vector $\mathrm{d} \in \mathbb{R}^m$ with $\mathrm{d}_k > 0, \forall k = 1, \cdots, m$, such that $\mathrm{g} = F_B(\mathrm{p}) = \left(\mathrm{diag}(\mathrm{d})^{-1} \otimes I_{\mathsf{d}}\right) \tilde{H}\mathrm{p}$.

Note that the condition $\mathrm{d}_k = \|\mathrm{z}_k\| = \|(H_k \otimes I_{\mathsf{d}})\mathrm{p}\|$ should be required for the components of the distance vector, where H_k is the k-th row from the incidence matrix H. Moreover, the vector in $\mathcal{Y}_{eq}(\mathcal{G}, g)$ can be generated from the space $\mathrm{Null}\left(\tilde{H}_{out}^T \mathrm{diag}(P_g)\right)$. Combining these conditions, it can be summarized that if there exists a configuration p satisfying

$$\mathrm{p} \in \mathrm{Null}\left(\tilde{H}_{out}^T \mathrm{diag}(P_g) \left(\mathrm{diag}(\mathrm{d})^{-1} \otimes I_{\mathsf{d}}\right) \tilde{H}\right), \tag{44}$$

then, the bearing vector $\mathrm{g} = F_B(\mathrm{p})$ is in the set $\mathcal{Y}(\mathcal{G}, g)$.

Lemma 13. *For the directed formation* $(\mathcal{G}, g)$ *over disordered LFF graph* $\mathcal{G}$*,*

$$\mathrm{Null}\left(\tilde{H}_{out}^T \mathrm{diag}(P_g) \left(\mathrm{diag}(\mathrm{d})^{-1} \otimes I_{\mathsf{d}}\right) \tilde{H}\right) = \mathrm{span}\{\mathbb{1}_n \otimes I_{\mathsf{d}}, p\}.$$

Proof. The Lemma 13 is dependent with two properties of the directed formation $(\mathcal{G}, g)$ over disordered LFF graph $\mathcal{G}$. The first one is that the directed formation $(\mathcal{G}, g)$ is IBR since the underlying graph $\mathcal{G}$ is generically bearing rigid and the bearing vector g is assumed to be not in the set of measure zero. In section 2.1, we showed that the following holds for IBR formation

$$\mathrm{Null}(\mathrm{diag}(P_g)\tilde{H}) = \mathrm{span}\{\mathbb{1}_n \otimes I_{\mathsf{d}}, p\}. \tag{45}$$

The second property of interest is the bearing kernel equivalence investigated by work [24], a brief introduction of this property can be found in Appendix C. The

main result of bearing kernel equivalent formation is discussed in Corollary 3. It can be summarized that for the formation $(\mathcal{G}, g)$ over disordered LFF graph,

$$\text{Null}(\tilde{H}_{out}^T \,\text{diag}(P_g)\tilde{H}) = \text{Null}(\text{diag}(P_g)\tilde{H}). \tag{46}$$

Then, some trick of linear algebra is applied here.

Corollary 2. *Suppose that $A \in \mathbb{R}^{p\times q}$, $C \in \mathbb{R}^{q\times p}$ and $B \in \mathbb{R}^{q\times q}$ is a full rank diagonal matrix. The following statements are equivalent:*

i) $\text{Null}(A) \bigcap \text{Range}(C) = \{\mathbb{0}_q\}$

ii) $\text{Null}(AC) = \text{Null}(C)$

iii) $\text{Null}(A) \bigcap \text{Range}(BC) = \{\mathbb{0}_q\}$

iv) $\text{Null}(ABC) = \text{Null}(BC)$

v) $\text{Null}(ABC) = \text{Null}(C)$

Proof. For any matrix multiplication AC, the null space of matrix AC can be expressed as the vector space $\text{Null}(AC) = \{x \in \mathbb{R}^p : ACx = \mathbb{0}_p\}$. Thus, the vector $x \in \text{Null}(AC)$ can be determined with two approaches. Firstly, any vector x in $\text{Null}(C)$ (i.e., $Cx = \mathbb{0}_q$) is also in $\text{Null}(AC)$ since $ACx = A\mathbb{0}_q = \mathbb{0}_p$. The second approach is that the vector x is in $\text{Null}(AC)$, if the vector $Cx \in \text{Range}(C)$ is also in $\text{Null}(A)$ (i.e., $A(Cx) = \mathbb{0}_p$).

($i \Leftrightarrow ii$) From the above paragraph, it can be inferred that $\text{Null}(C) \subseteq \text{Null}(AC)$. Moreover, $\text{Null}(C) = \text{Null}(AC)$ if and only if no vector can be generated from the second approach, or mathematically, $\text{Null}(A) \bigcap \text{Range}(C) = \{\mathbb{0}_q\}$.

($iii \Leftrightarrow iv$) The proof is exactly the same as ($i \Leftrightarrow ii$).

($i \Leftrightarrow iii$) Since the matrix B is a full rank diagonal matrix, it can be obtained that $\text{Range}(C) = \text{Range}(BC)$. Therefore, $\text{Null}(A) \bigcap \text{Range}(C)$ equals to $\text{Null}(A) \bigcap \text{Range}(BC)$ and statement i is equivalent to statement iii.

($iv \Leftrightarrow v$) Since the matrix B is a full rank diagonal matrix, its null space $\text{Null}(B) = \{\mathbb{0}_q\}$. Then, $\text{Null}(B) \bigcap \text{Range}(C) = \{\mathbb{0}_q\}$ always holds. As proved ($i \Leftrightarrow ii$), this implies $\text{Null}(BC) = \text{Null}(C)$ is always true. So the statement iv ($\text{Null}(ABC) = \text{Null}(BC)$) is equivalent to statement v ($\text{Null}(ABC) = \text{Null}(C)$). □

Recall in Corollary 3 and Equation (46), the directed formation over disordered LFF graph is bearing kernel equivalent, meaning that $\text{Null}\left(\tilde{H}_{out}^T \,\text{diag}(P_g)\tilde{H}\right) = \text{Null}\left(\text{diag}(P_g)\tilde{H}\right)$. It coincides with the statement (ii) where matrix $A = \tilde{H}_{out}^T \in \mathbb{R}^{nd\times md}$ and $C = \left(\text{diag}(P_g)\tilde{H}\right) \in \mathbb{R}^{md\times nd}$. Let the matrix $\left(\text{diag}(d)^{-1} \otimes I_{\mathsf{d}}\right)$ which is a

full rank diagonal matrix in $\mathbb{R}^{md\times md}$ take the role as $\boldsymbol{B}$. With the statement (v), it can be inferred that

$$\text{Null}\left(\tilde{H}_{out}^T\left(\text{diag}(d)^{-1}\otimes I_{\mathsf{d}}\right)\text{diag}(P_g)\tilde{H}\right)=\text{Null}\left(\text{diag}(P_g)\tilde{H}\right) \tag{47}$$

Moreover, the matrix $\left(\text{diag}(d)^{-1}\otimes I_{\mathsf{d}}\right)$ and matrix $\text{diag}(P_g)$ commute, since both matrices are symmetric and their product is also symmetric (the product of a diagonal matrix and a symmetric matrix is symmetric). Thus, we can switch their position in matrix multiplication, i.e.,

$$\tilde{H}_{out}^T\left(\text{diag}(d)^{-1}\otimes I_{\mathsf{d}}\right)\text{diag}(P_g)\tilde{H}=\tilde{H}_{out}^T\,\text{diag}(P_g)\left(\text{diag}(d)^{-1}\otimes I_{\mathsf{d}}\right)\tilde{H}. \tag{48}$$

With the equations (45), (47), (48), it can be proved that

$$\text{Null}\left(\tilde{H}_{out}^T\,\text{diag}(P_g)\left(\text{diag(d)}^{-1}\otimes I_{\mathsf{d}}\right)\tilde{H}\right)=\text{span}\{\mathbb{1}_n\otimes I_{\mathsf{d}},p\}.$$

□

With Lemma 13, the configuration p satisfying condition (44) can be determined in the subspace $\text{span}\{\mathbb{1}_n\otimes I_{\mathsf{d}},p\}$. Furthermore, the bearing vector in the set $\mathcal{Y}(\mathcal{G},g)$ can be found by $\text{g}=F_B(\text{p})$. For any configuration p in $\text{span}\{\mathbb{1}_n\otimes I_{\mathsf{d}},p\}$, the bearing function will lead to $\text{g}=F_B(\text{p})=\pm g$. Therefore, the bearing vectors g and $-g$ are the only elements in the equilibrium set $\mathcal{Y}(\mathcal{G},g)$. Followed by that, the Lemma 12 refers that the equilibrium set

$$\mathcal{X}(\mathcal{G},\text{g})=\{\text{g},-\text{g}\}.$$

As we discussed, the configuration p corresponding to the bearing vector can be uniquely determined according to the HCLFF subgraph and the initial condition of p_1,d_{21}. We denote p_a^* and p_b^* as the equilibrium configuration satisfying bearing vector g and −g separately.

Lemma 14. *For the bearing-only formation control system* (13) *with directed sensing described with disordered LFF graph (Def. 13), the equilibrium p_b^* is unstable.*

Proof. The stability of equilibrium p_b^* can be proved with stability theorem of cascade structure. With a leader and a first follower, the nonlinear control system can be separated into two subsystems,

$$\begin{bmatrix}\dot{p}_1\\ \dot{p}_2\end{bmatrix}=\begin{bmatrix}u_1(p_1)\\ u_2(p_1,p_2)\end{bmatrix} \tag{49}$$

$$\begin{bmatrix}\dot{p}_3\\ \vdots\\ \dot{p}_n\end{bmatrix}=\begin{bmatrix}u_3(p_1,p_2,p_3,\cdots,p_n)\\ \vdots\\ u_n(p_1,p_2,p_3,\cdots,p_n)\end{bmatrix}. \tag{50}$$

The configuration $p_b^* = [p_1^{*T}, p_{2b}^{*\ T}, p_{3b}^{*\ T}, \cdots, p_{nb}^{*\ T}]^T$ is one of the equilibrium of the whole system. The part $[p_1^{*T}, p_{2b}^{*\ T}]^T$ is one of the equilibrium of system (49). And the rest part $[p_{3b}^{*\ T}, \cdots, p_{nb}^{*\ T}]^T$ is the equilibrium of system (50) with p_1, p_2 fixed at p_1^*, p_{2b}^*.

From the stability theorem of cascade structure, the equilibrium p_b^* is GAS, if $[p_1^{*T}, p_{2b}^{*\ T}]^T$ is GAS for system (49) and $[p_{3b}^{*\ T}, \cdots, p_{nb}^{*\ T}]^T$ is GAS for system (50) with p_1, p_2 fixed at p_1^*, p_{2b}^*. However, the Lemma 4 shows that the equilibrium $[p_1^{*T}, p_{2b}^{*\ T}]^T$ is not stable for system (49). So the configuration p_b^* is not stable for the whole system. □

To find the convergence of bearing-only formation control system with disordered LFF sensing graph, we still need to determine the stability of the other equilibrium p_a^*.

Conjecture 1. *For the bearing-only formation control system* (13) *with directed sensing described with disordered LFF graph (Def. 13), the configuration at equilibrium p_a^* is almost globally asymptotically stable.*

Unfortunately, we didn't manage to find the appropriate way to prove this conjecture mathematically. Since the cascade structure does not appear in the bearing-only formation control system with disordered LFF sensing graph, we can not apply the theorem of cascade system (Theorem 6) to prove Conjecture 1. Thus, the preferable method is prove with a suitable Lyapunov function. This method should work, but it is difficult since the BOFC system (13) with directed sensing is strongly nonlinear and asymmetric.

In the following, we show by example that Conjecture 1 seems to hold.

Example 10. *For this numerical simulation, the target formation is assigned as Figure 26a. The directed sensing condition is expressed by a disordered LFF graph shown as the underlying graph of the target formation. The initial configuration of*

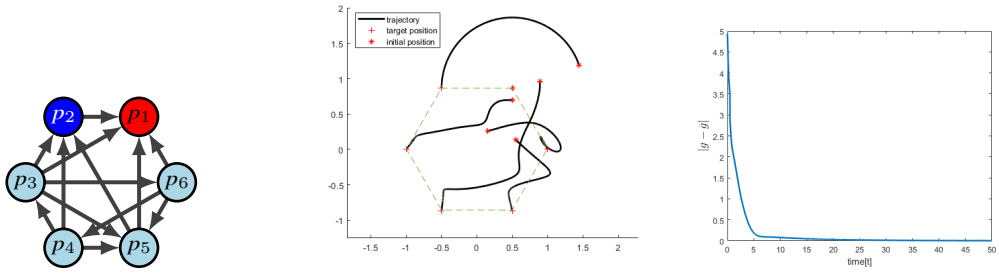

(a) The target bearing formation.

(b) System trajectories.

(c) Bearing error along the system trajectories.

Figure 26: Simulation result of bearing-only formation control system with target bearing formation as Figure 26a.

the system is chosen randomly. For this particular example,

$$p(t_0) = [(0.5000, 0.8660), (1.4469, 1.1875), (0.5060, 0.6991), \\ (0.8909, 0.9593), (0.5472, 0.1386), (0.1493, 0.2575)]^T.$$

The agents in the system are controlled with bearing-only formation control with directed sensing (12)*. As shown in Figure 26b, the MAS converges to the target bearing formation, which coincides with the equilibrium* p_a^**. Moreover, the Figure 25c indicates that the bearing error between the target bearing and current bearing converges to zero asymptotically.*

As a conclusion, the bearing-only formation control system with the disordered directed sensing has exactly two equilibrium. The undesired equilibrium is unstable, while the desired equilibrium seems to be asymptotically stable.

4 Conclusion and Open Questions

In this chapter, we conclude the work conducted for this thesis and also suggest some future orientation following our results.

4.1 Conclusion

In Section 3.3, we presented the 1-to-many control system which is a simpler bearing-only formation control problem with directed sensing. The analysis of the motion was performed according to different numbers of outgoing edges. We proposed the scheme to work out the equilibrium for the nonlinear bearing-only formation control system. The result is that in the 1-to-many system with arbitrary leaders, the follower agent asymptotically converges to the position satisfying the target bearing.

In Section 3.4, we discussed some different approaches for expansion of directed sensing graph such that the bearing-only formation control still works. We firstly extended the HCLFF graph to ordered LFF graph (Def. 12) with the orderliness in structure maintained. The stability theorem of cascade nonlinear system helps to simplify the convergence analysis of the BOFC system. Then, we proposed the disordered LFF graph (Def. 13) which breaks the orderliness. The equilibrium analysis was performed with the similar method as 1-to-many system. Although the stability of system equilibrium was partially determined, we provided some simulation results showing that the disordered LFF graph actually solves the main problem of this research (Problem 3). As a result, the BOFC system with either ordered LFF sensing graph or disordered LFF sensing graph converges asymptotically to the target formation from almost every initial conditions.

4.2 Open Questions

In Section 3.4, the research focuses on the condition of graph with a leader and a first follower which helps to uniquely define the configuration satisfying the target formation. The situation that the graph does not contain a leader and a first follower is still an open question. The ultimate target of this thesis is to determine whether the bearing-only formation control can drive the system to the target formation with an arbitrary directed sensing graph. In this direction, the future work can focus on the problem with varying (or dynamic) sensing condition. Extra control effort may be utilized on the sensors of agents to hold the sensing condition inside the class that bearing-only formation control works. The work [28] offers an example on the MAS with two agents.

On the theoretical side, we suggest that common conditions for the directed graphs is generically bearing rigidity and bearing kernel equivalence. The existing works presented that the leader-first-follower graph generated from Henneberg construction is a basic graph satisfying these two common conditions. Actually, these conditions belong to the bearing rigidity theory on directed graphs. Although the bearing rigidity theory has been developed completely on undirected graphs as

introduced in Section 2.1, the theory on directed graphs is not well-defined.

Finally, in this work we illustrated that for bearing-only formation control system with disordered LFF graph, the equilibrium corresponding to the target formation is the only equilibrium possible to be stable. The simulations also implied that the system would converge to the target bearing. The relating proof should be given in future work.

Appendices

A Stability of Cascade Dynamical Systems

The stability of cascade dynamical system sis widely applied in control theory. In this section, we summarize the version presented in [36, Thm 4.1]. Consider the nonlinear triangular system

$$\dot{x} = f(x) \tag{51}$$

$$\dot{y} = g(x, y), \tag{52}$$

where the variables $x \in \mathbb{R}^k$; $y \in \mathbb{R}^m$ and the functions $f : \mathbb{R}^k \to \mathbb{R}^k$, $g : \mathbb{R}^{n=k+m} \to \mathbb{R}^m$. The variable of the space $\mathbb{R}^n = \mathbb{R}^{k+m}$ is denoted by $z = [x^T, y^T]^T$. It is assumed that the function f and g satisfy local Lipschitz conditions and that all solutions exist $\forall t \geq 0$.

Suppose that $f(x^*) = 0$, implying that x^* is an equilibrium of subsystem (51). Then, fix $x = x^*$ in subsystem (52) as follows,

$$\dot{y} = g(x^*, y). \tag{53}$$

Denote y^* as the equilibrium of system (53), satisfying $g(x^*, y^*) = 0$. Then, $z^* = [x^{*T}, y^{*T}]^T$ will be an equilibrium of system (51) and (52).

Theorem 6. *If x^* is global asymptotically stable(GAS) for (51) and y^* is GAS for system (53), then z^* is GAS for the triangular system (51) and (52).*

The proof of the theorem can be accessed by Lyapunov function techniques [37].

B Proof of the Equilibrium Analysis of 1-to-many System with One or Two Outgoing Edges

B.1 One Outgoing Edge Case

In the case that there is only one leader for the controllable agent, the control system can be expressed as:

$$\dot{p}_c = -P_{g_{c1}} \mathrm{g}_{c1} \tag{54}$$

The equilibrium analysis has been well performed in [29]. The result is described in lemma 4. The detailed proof is shown below.

Proof. First, we can verify the invariance of d_{c1} along the system trajectories. Consider its derivative,

$$\begin{aligned} \frac{d}{dt} d_{c1}^2 &= \frac{d}{dt}(z_{c1}^T z_{c1}) \\ &= 2 z_{c1}^T \dot{z}_{c1} \\ &= 2 z_{c1}^T (\dot{p}_1 - \dot{p}_c) \\ &= 2 z_{c1}^T P_{g_{c1}} \mathrm{g}_{c1} \\ &= 0. \end{aligned} \tag{55}$$

Consequently, d_{c1} is not varying, or equivalently, the trajectory of agent c should belong to a circle with radius d_{c1} and center p_1.

With the system stated in (54), the equilibrium is reached when $\dot{p}_c = -P_{g_{c1}} \mathrm{g}_{c1} = 0$. The property of projection matrix implies that

$$g_{c1}^* = \pm \mathrm{g}_{c1}. \tag{56}$$

Along with the conclusion on the trajectory of agent c, there exists two equilibrium. The first equilibrium $p_{ca}^* = p_1 - d_{c1}\mathrm{g}_{c1}$ satisfies the condition $g_{c1}^* = \mathrm{g}_{c1}$, meaning that the bearing measurement reaches the target. Thus, p_{ca}^* is denoted as the desired equilibrium. The second equilibrium $p_{cb}^* = p_1 + d_{c1}\mathrm{g}_{c1}$ satisfies the condition $g_{c1}^* = -\mathrm{g}_{c1}$, which is not desired in the formation control problem (Problem 2).

Consider the Lyapunov function $V_a = \frac{1}{2}||p_c - p_{ca}^*||^2$ and $V_b = \frac{1}{2}||p_c - p_{cb}^*||^2$. It can be verified that V_a and V_b are positive semi-definite. The Lyapunov function equals to zero ($V_a = 0$ or $V_b = 0$) if and only if agent v_c locates on the corresponding

equilibria ($p_c = p^*_{ca}$ or $p_c = p^*_{cb}$). Along a trajectory of system (54),

$$\begin{aligned}\dot{V}_a &= (p_c - p^*_{ca})^T \dot{p}_c \\ &= -(p_c - p^*_{ca})^T P_{g_{c1}} \mathrm{g}_{c1} \\ &= -[(p_c - p_1) + (p_1 - p^*_{ca})]^T P_{g_{c1}} \mathrm{g}_{c1} \\ &= -(p_1 - p^*_{ca})^T P_{g_{c1}} \mathrm{g}_{c1} \\ &= -d_{c1} (\mathrm{g}^*_{c1})^T P_{g_{c1}} \mathrm{g}_{c1} \leq 0\end{aligned} \tag{57}$$

Similarly,

$$\dot{V}_b = d_{c1} (\mathrm{g}^*_{c1})^T P_{g_{c1}} \mathrm{g}_{c1} \geq 0. \tag{58}$$

The last inequality holds since the projection matrix is always positive definite. $\dot{V}_a = 0$ if and only if $p_c = p^*_{ca}$ or $p_c = p^*_{cb}$. Thus, p^*_{cb} is unstable and p^*_{ca} is almost globally asymptotically stable due to LaSalle's principle.

□

B.2 Two Outgoing Edge Case

With two outgoing edges (pointing to agents v_1 and v_2), the dynamics of agent v_c can be expressed as

$$\dot{p}_c = -P_{g_{c1}} \mathrm{g}_{c1} - P_{g_{c2}} \mathrm{g}_{c2}. \tag{59}$$

As before, the system convergence is concluded in Lemma 5.

Proof. The equilibrium of the system should satisfy

$$-P_{g^*_{c1}} \mathrm{g}_{c1} - P_{g^*_{c2}} \mathrm{g}_{c2} = 0 \tag{60}$$

By multiplying $-g^{*T}_{c1}$ on the left, we have $g^{*T}_{c1} \left(P_{g^*_{c1}} \mathrm{g}_{c1} + P_{g^*_{c2}} \mathrm{g}_{c2} \right) = g^{*T}_{c1} P_{g^*_{c2}} \mathrm{g}_{c2} = 0$. This equation holds if and only if $g^*_{c1} = \pm g^*_{c2}$ or $g^*_{c2} = \pm \mathrm{g}_{c2}$. The first condition $g^*_{c1} = \pm g^*_{c2}$ can be satisfied unless g_{c1} is parallel with g_{c2}, which contradicts with assumption **??**. On the other hand, $g^*_{c1} = \pm \mathrm{g}_{c1}$ can be obtained by substituting the second condition $g^*_{c2} = \pm \mathrm{g}_{c2}$ back to (60). Thus, the equilibrium condition for equation (60) can be simplified as:

$$g^*_{c1} = \pm \mathrm{g}_{c1}, g^*_{c2} = \pm \mathrm{g}_{c2} \tag{61}$$

Geometrically, $g^*_{c1} = \mathrm{g}_{c1}$ and $g^*_{c2} = \mathrm{g}_{c2}$ is the only realizable combination in $\mathbb{R}^d$. Then, we can locate the equilibrium p^*_c at $(P_{\mathrm{g}_{c1}} + P_{\mathrm{g}_{c2}})^{-1} (P_{\mathrm{g}_{c1}} p_1 + P_{\mathrm{g}_{c2}} p_2)$.

Consider the Lyapunov function $V = \frac{1}{2}||p_c - p_c^*||^2$, which is positive definite, radially bounded and continuously differentiable. Along the trajectory, we have

$$\begin{aligned}
\dot{V} &= (p_c - p_c^*)^T \dot{p}_c \\
&= -(p_c - p_c^*)^T (P_{g_{c1}} g_{c1} + P_{g_{c2}} g_{c2}) \\
&= -(p_c - p_c^*)^T \left(\frac{P_{g_{c1}}}{d_{c1}^*} z_{c1}^* + \frac{P_{g_{c2}}}{d_{c2}^*} z_{c2}^* \right) \\
&= -(p_c - p_c^*)^T \left[\frac{P_{g_{c1}}}{d_{c1}^*} (p1 - p_c + p_c - p_c^*) + \frac{P_{g_{c2}}}{d_{c2}^*} (p2 - p_c + p_c - p_c^*) \right] \\
&= -(p_c - p_c^*)^T \left(\frac{P_{g_{c1}}}{d_{c1}^*} + \frac{P_{g_{c2}}}{d_{c2}^*} \right) (p_c - p_c^*) \leq 0
\end{aligned} \tag{62}$$

The inequality holds since $\left(\frac{P_{g_{c1}}}{d_{c1}^*} + \frac{P_{g_{c2}}}{d_{c2}^*} \right)$ is positive semi-definite. Moreover, $\dot{V} = 0$ if and only if when the system reaches equilibrium (i.e., $p_c = p_c^*$). (A relating proof can be found in [29], it is also similar with the proof of Lemma 10. □

C Bearing Kernel Equivalence of Directed Formations

The work [24] focuses on a property of directed formations called *bearing kernel equivalence*. The notion of bearing equivalence emerges as one of the key properties to critically affect stability and convergence of bearing-based formation systems (defined in the following paragraphs) modelled by directed graphs.

In this research, the bearing kernel equivalence is applied to prove Lemma 13. In this section, we will briefly define this property. The introduction starts from the bearing-based formation control system with undirected sensing,

$$\dot{p}_i = u_i = -\sum_{j \in \mathcal{N}_i} P_{g_{ij}}(p_i - p_j). \tag{63}$$

Its matrix form is expressed as,

$$\dot{p} = u = -L_B p, \tag{64}$$

where $L_B = \tilde{H}^T \operatorname{diag}(P_g)\tilde{H}$ is called the *bearing Laplacian* matrix over undirected formation $(\mathcal{G}, g)$.

In the work [17], they showed that the bearing-based formation control strategy (64) solves the bearing formation control problem with undirected sensing (Problem 1) mainly because

$$\operatorname{Null}(L_B) = \operatorname{Null}(R_B) = \operatorname{span}\{\mathbb{1}_n \otimes I_{\mathsf{d}}, p\}. \tag{65}$$

As we introduced in Section 2.2, the bearing-only formation control 11 also solves the bearing formation control problem with undirected sensing (Problem 1). These main differences between these two control strategies are *i*) BOFC requires only the bearing measurement, while the bearing-based formation control applies the relative position measurement as well; *ii*) BOFC is a nonlinear control scheme, but the bearing-based formation control is linear.

Later, the bearing-based formation control system was also developed for directed sensing graphs,

$$\dot{p} = u = -\bar{L}_B p, \tag{66}$$

where $\bar{L}_B = \tilde{H}_{out}^T \operatorname{diag}(P_g)\tilde{H}$ is the bearing Laplacian matrix over directed formation $(\mathcal{G}, g)$. In the work [24], they pointed out that the key to determine whether bearing-based formation control strategy (66) solves the bearing formation control problem with directed sensing (Problem 4) is if the bearing Laplacian matrix over directed formation $\bar{L}_B$ satisfies the kernel space condition (65) like the undirected version. Thus, they define the bearing kernel equivalence as following:

Definition 14 ([24]). *A directed formation $(\mathcal{G}, g)$ is bearing kernel equivalent if* $\operatorname{Null}(\bar{L}_B) = \operatorname{Null}(R_B) = \operatorname{span}\{\mathbb{1}_n \otimes I_{\mathsf{d}}, p\}$.

The work [24] then proposed some conditions for the formations to be bearing kernel equivalent.

Corollary 3 ([24])**.** *The directed formations over disordered LFF graphs are bearing kernel equivalent, i.e.,*

$$\mathrm{Null}(\bar{L}_B) = \mathrm{Null}(R_B) = \mathrm{span}\{\mathbb{1}_n \otimes I_{\mathsf{d}}, p\}.$$

Or equivalently,

$$\mathrm{Null}(\tilde{H}_{out}^T \,\mathrm{diag}(P_g)\tilde{H}) = \mathrm{Null}(\mathrm{diag}(P_g)\tilde{H}) = \mathrm{span}\{\mathbb{1}_n \otimes I_{\mathsf{d}}, p\}.$$

The presented Corollary 3 was one of the results concluded in [24]. With this corollary, we can prove the Lemma 13.

References

[1] B. Burmeister, A. Haddadi, and G. Matylis, "Application of multi-agent systems in traffic and transportation," *IEE Proceedings-Software Engineering*, vol. 144, no. 1, pp. 51–60, 1997.

[2] S. D. McArthur, E. M. Davidson, V. M. Catterson, A. L. Dimeas, N. D. Hatziargyriou, F. Ponci, and T. Funabashi, "Multi-agent systems for power engineering applications—part i: Concepts, approaches, and technical challenges," *IEEE Transactions on Power systems*, vol. 22, no. 4, pp. 1743–1752, 2007.

[3] ——, "Multi-agent systems for power engineering applications—part ii: Technologies, standards, and tools for building multi-agent systems," *IEEE Transactions on Power Systems*, vol. 22, no. 4, pp. 1753–1759, 2007.

[4] S. Das, D. Goswami, S. Chatterjee, and S. Mukherjee, "Stability and chaos analysis of a novel swarm dynamics with applications to multi-agent systems," *Engineering Applications of Artificial Intelligence*, vol. 30, p. 189–198, Apr. 2014.

[5] M. A. Lewis and K.-H. Tan, "High precision formation control of mobile robots using virtual structures," *Autonomous robots*, vol. 4, pp. 387–403, 1997.

[6] W. Ren, "Consensus based formation control strategies for multi-vehicle systems," in *2006 American Control Conference*. IEEE, 2006.

[7] D. Xu, X. Zhang, Z. Zhu, C. Chen, and P. Yang, "Behavior-based formation control of swarm robots," *Mathematical Problems in Engineering*, vol. 2014, p. 1–13, 2014.

[8] W. Ren and E. Atkins, "Distributed multi-vehicle coordinated control via local information exchange," *International Journal of Robust and Nonlinear Control*, vol. 17, no. 10–11, p. 1002–1033, Nov. 2006.

[9] H. G. de Marina, "Maneuvering and robustness issues in undirected displacement-consensus-based formation control," *IEEE Transactions on Automatic Control*, vol. 66, no. 7, p. 3370–3377, Jul. 2021.

[10] K.-K. Oh and H.-S. Ahn, "Formation control of mobile agents based on inter-agent distance dynamics," *Automatica*, vol. 47, no. 10, p. 2306–2312, Oct. 2011.

[11] S. Zhao and D. Zelazo, "Bearing rigidity and almost global bearing-only formation stabilization," *IEEE Transactions on Automatic Control*, vol. 61, no. 5, p. 1255–1268, May 2016.

[12] L. Krick, M. E. Broucke, and B. A. Francis, "Stabilisation of infinitesimally rigid formations of multi-robot networks," *International Journal of Control*, vol. 82, no. 3, p. 423–439, Feb. 2009.

[13] K.-K. Oh and H.-S. Ahn, "Distance-based undirected formations of single-integrator and double-integrator modeled agents in n -dimensional space: Distance-based undirected formations," *International Journal of Robust and Nonlinear Control*, vol. 24, no. 12, p. 1809–1820, Jan. 2013.

[14] Z. Sun, S. Mou, M. Deghat, B. Anderson, and A. Morse, "Finite time distance-based rigid formation stabilization and flocking," *IFAC Proceedings Volumes*, vol. 47, no. 3, p. 9183–9189, 2014.

[15] R. Olfati-Saber and R. Murray, "Graph rigidity and distributed formation stabilization of multi-vehicle systems," in *Proceedings of the 41st IEEE Conference on Decision and Control, 2002.*, ser. CDC-02. IEEE.

[16] B. D. Anderson, C. Yu, B. Fidan, and J. M. Hendrickx, "Rigid graph control architectures for autonomous formations," *IEEE Control Systems Magazine*, vol. 28, no. 6, pp. 48–63, 2008.

[17] S. Zhao and D. Zelazo, "Bearing-based distributed control and estimation of multi-agent systems," in *2015 European Control Conference (ECC)*. IEEE, Jul. 2015.

[18] T. Eren, "Formation shape control based on bearing rigidity," *International Journal of Control*, vol. 85, no. 9, p. 1361–1379, Sep. 2012.

[19] X. Li, X. Luo, J. Wang, Y. Zhu, and X. Guan, "Bearing-based formation control of networked robotic systems with parametric uncertainties," *Neurocomputing*, vol. 306, p. 234–245, Sep. 2018.

[20] A. Cornejo, A. J. Lynch, E. Fudge, S. Bilstein, M. Khabbazian, and J. McLurkin, "Scale-free coordinates for multi-robot systems with bearing-only sensors," *The International Journal of Robotics Research*, vol. 32, no. 12, p. 1459–1474, Oct. 2013.

[21] S. Zhao and D. Zelazo, "Bearing-based formation maneuvering," in *2015 IEEE International Symposium on Intelligent Control (ISIC)*. IEEE, Sep. 2015.

[22] ——, "Localizability and distributed protocols for bearing-based network localization in arbitrary dimensions," *Automatica*, vol. 69, p. 334–341, Jul. 2016.

[23] ——, "Bearing-based formation stabilization with directed interaction topologies," in *2015 54th IEEE Conference on Decision and Control (CDC)*. IEEE, Dec. 2015.

[24] Z. Sun, S. Zhao, and D. Zelazo, "Characterizing bearing equivalence in directed graphs," *IFAC-PapersOnLine*, vol. 56, no. 2, p. 3788–3793, 2023.

[25] M. Basiri, A. N. Bishop, and P. Jensfelt, "Distributed control of triangular formations with angle-only constraints," *Systems amp; Control Letters*, vol. 59, no. 2, p. 147–154, Feb. 2010.

[26] A. Franchi, C. Masone, V. Grabe, M. Ryll, H. H. Bülthoff, and P. R. Giordano, "Modeling and control of uav bearing formations with bilateral high-level steering," *The International Journal of Robotics Research*, vol. 31, no. 12, p. 1504–1525, Oct. 2012.

[27] A. Franchi and P. R. Giordano, "Decentralized control of parallel rigid formations with direction constraints and bearing measurements," in *2012 IEEE 51st IEEE Conference on Decision and Control (CDC)*. IEEE, Dec. 2012.

[28] D. Frank, D. Zelazo, and F. Allgöwer, "Bearing-only formation control with limited visual sensing: Two agent case," *IFAC-PapersOnLine*, vol. 51, no. 23, p. 28–33, 2018.

[29] M. H. Trinh, S. Zhao, Z. Sun, D. Zelazo, B. D. Anderson, and H.-S. Ahn, "Bearing-based formation control of a group of agents with leader-first follower structure," *IEEE Transactions on Automatic Control*, p. 1–1, 2018.

[30] T. Eren, W. Whiteley, A. Morse, P. Belhumeur, and B. Anderson, "Sensor and network topologies of formations with direction, bearing and angle information between agents," in *42nd IEEE International Conference on Decision and Control (IEEE Cat. No.03CH37475)*, ser. CDC-03. IEEE.

[31] D. Zelazo, A. Franchi, and P. R. Giordano, "Rigidity theory in se(2) for unscaled relative position estimation using only bearing measurements," in *2014 European Control Conference (ECC)*. IEEE, Jun. 2014.

[32] S. Zhao, Z. Sun, D. Zelazo, M.-H. Trinh, and H.-S. Ahn, "Laman graphs are generically bearing rigid in arbitrary dimensions," in *2017 IEEE 56th Annual Conference on Decision and Control (CDC)*. IEEE, Dec. 2017.

[33] G. Michieletto, A. Cenedese, and A. Franchi, "Bearing rigidity theory in se(3)," in *2016 IEEE 55th Conference on Decision and Control (CDC)*. IEEE, Dec. 2016.

[34] M. Mesbahi and M. Egerstedt, *Graph Theoretic Methods in Multiagent Networks*. Princeton University Press, Dec. 2010.

[35] *Rigidity Theory and Applications*. Kluwer Academic Publishers, 2002.

[36] P. Seibert and R. Suarez, "Global stabilization of nonlinear cascade systems," *Systems amp; Control Letters*, vol. 14, no. 4, p. 347–352, Apr. 1990.

[37] M. Vidyasagar, "Decomposition techniques for large-scale systems with nonadditive interactions: Stability and stabilizability," *IEEE Transactions on Automatic Control*, vol. 25, no. 4, p. 773–779, Aug. 1980.

Hebrew Abstract

תזה זו חוקרת את הבעיה של בקרת תצורה, שמטרתה להניע מערכת מרובת סוכנים להשיג תצורה מרחבית רצויה. מוצעת סכמת שליטה שנקראת בקרת תצורה על סמך זוויות לפתרון הבעיה הזו. הבקר הזה קיבל עניין מחקרי מכיוון שהוא דורש ומחיל רק מדידות זוויות בין הסוכנים, במקום מדידות מרחק.

אחת מההגבלות של בקרת תצורה על סמך זוויות הינו תנאי החישה שננקוב בו. עבודות ראשונות חקרו מקיפית את הבקר הזה בהנחה על חישה לא מופנה בין הסוכנים, שנחשב כתנאי לא ריאליסטי. מאמץ מחקרי יותר עדכני התמקד בבעיה עם חישה מופנה, כאשר אך לא בהכרח להפך. מחקר חדש הראה כי החוק לשליטה j יכול לחוש את הסוכן i הסוכן על פי זוויות בלבד עובד גם עם קובצה מסוימת של גרפים של חישה מופנה שנקראים על סמך זוויות בלבד.. זהו צעד Henneberg שנוצרים מבניית (LFF) ""מנהיג-ראשון-עוקב מהותי הלאה מההנחה הקודמת של גרפים לא מופנוים למשפחת גרפים מופנים מצומצמת. על בסיס זה, המטרה של העבודה היא להרחיב את התוצאות לתנאים כלליים יותר על מגרפי חישה מופנות שבהן בקרת הזוויות בלבד מצליחה.

על מנת להשיג זאת, אנו ננתח תחילה מערכת מרובת סוכנים עם סוכן נע יחיד שמבוקר על סמך זוויות בלבד. המטרה היא לקבוע האם הסוכן הנע יתכנס למיקום רצוי המקיים את כל הזוויות המטרה המצוינות, למספרים שונים של קשתות יוצאות (סוכנים שהוא יכול לחוש). האתגר העיקרי הוא למצוא נקודות שיווי משקל של מערכת לא לינארית זו. הגישה שלנו מתמקדת בניתוח של בעיה לינארית קשורה וביצוע הקישור לנקודות שיווי משקל של המערכת הלא לינארית. לאחר הגדרת נקודות השיווי משקל של המערכת, אנו מבצעים גם ניתוח יציבות המראה כי הסוכן הנע מתכנס למיקום הרצוי. תוצאה זו מאפשרת לנו להרחיב שבהן לסוכנים עוקבים יכולים LFF את משפחת הגרפים שפותרות את הבעיה לגרפים להיות יותר מ-2 קשתות חיישה יוצאות. אנו מבצעים ניתוחי יציבות והתכנסות עבור מקרה זה. אנו חוקרים גם הרחבה נוספת של משפחת הגרפים ונניח כי תנאי מספיק לפתרון בעיית הנחה זו מאומתת .LFF בקרת התצורה כללית יותר הוא שיש קיום תת-גרף שהוא גרף באמצעות בסימולציות.

המחקר בוצע בהנחייתו של פרופסור דניאל זלזו, בפקולטה מערכות אוטונומיות ורובוטיקה.

מחבר/ת חיבור זה מצהיר/ה כי המחקר, כולל איסוף הנתונים, עיבודם והצגתם, התייחסות והשוואה למחקרים
קודמים וכו', נעשה כולו בצורה ישרה, כמצופה ממחקר מדעי המבוצע לפי אמות המידה האתיות של העולם
האקדמי. כמו כן, הדיווח על המחקר ותוצאותיו בחיבור זה נעשה בצורה ישרה ומלאה, לפי אותן אמות מידה.

אני מודה לטכניון על התמיכה הכספית הנדיבה בהשתלמותי.

בקרת מבנה לפי זוויות כיוון
על ידי חישה כיוונית

חיבור על מחקר

לשם מילוי חלקי של הדרישות לקבלת התואר מגיסטר למדעים ב

מערכות אוטונומיות ורובוטיקה

שי צויצן

הוגש לסנט הטכניון - מכון טכנולוגי לישראל

חיפה

ניסן 5784, אפריל 2024